Frank Laboratory of Neutron Physics
Joint Institute for Nuclear Research

Current state of the FSD diffractometer

G.D. Bokuchava

49th meeting of the PAC for Condensed Matter Physics, 24-25 January 2019

IBR-2 pulsed reactor in FLNP JINR

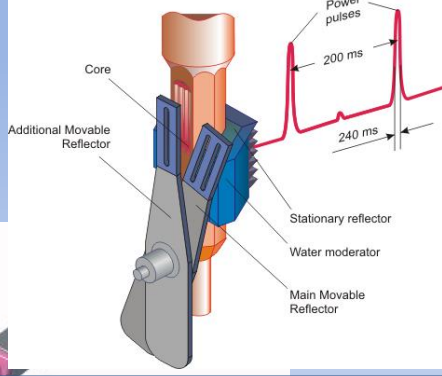

Neutron flux: ~10^{16} n/cm^{2}s
Pulse repetition rate: 5 Hz
Thermal neutron
pulse width: 340 μs

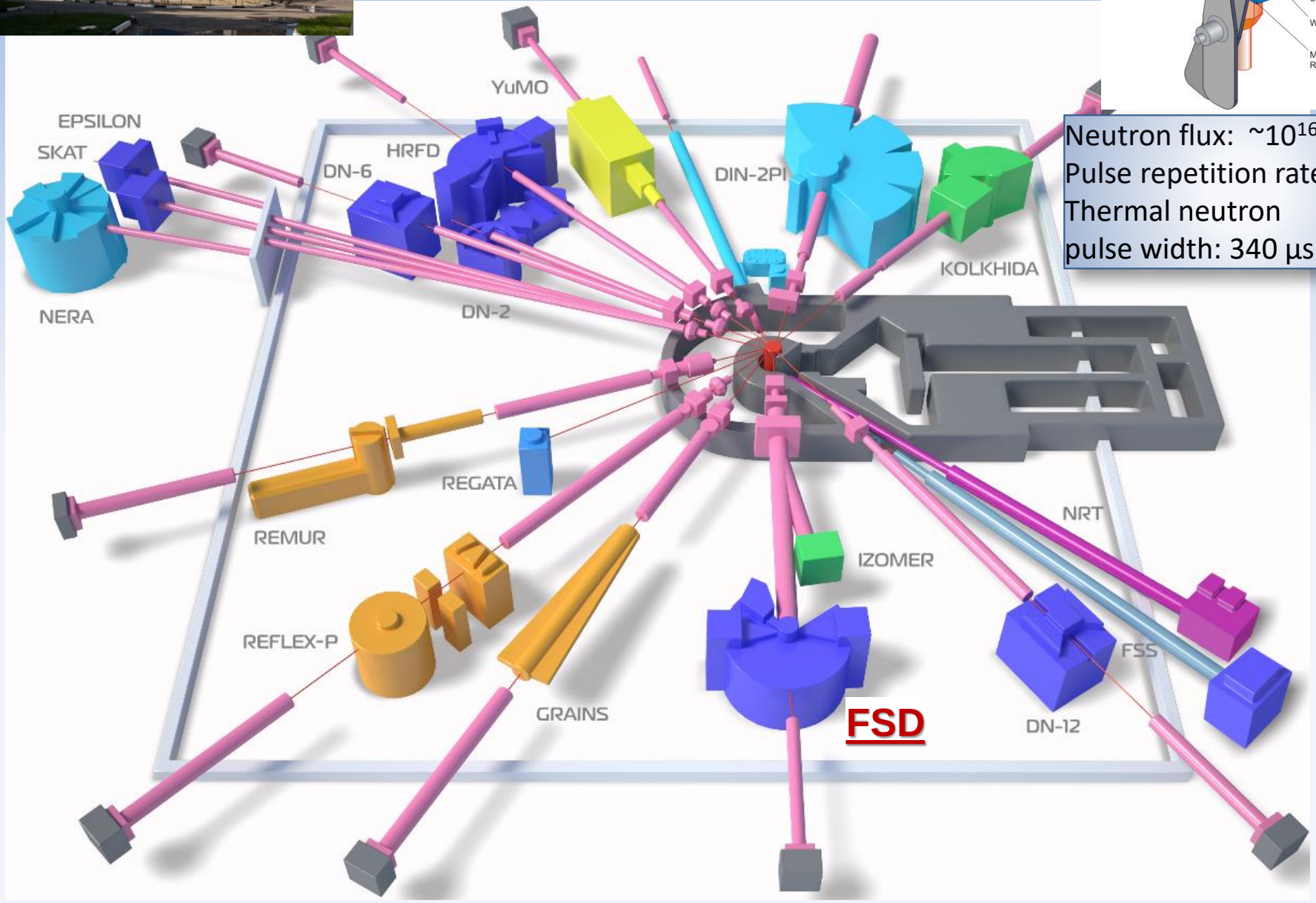

FSD – Fourier Stress Diffractometer at the IBR-2 pulsed reactor (JINR, Dubna)

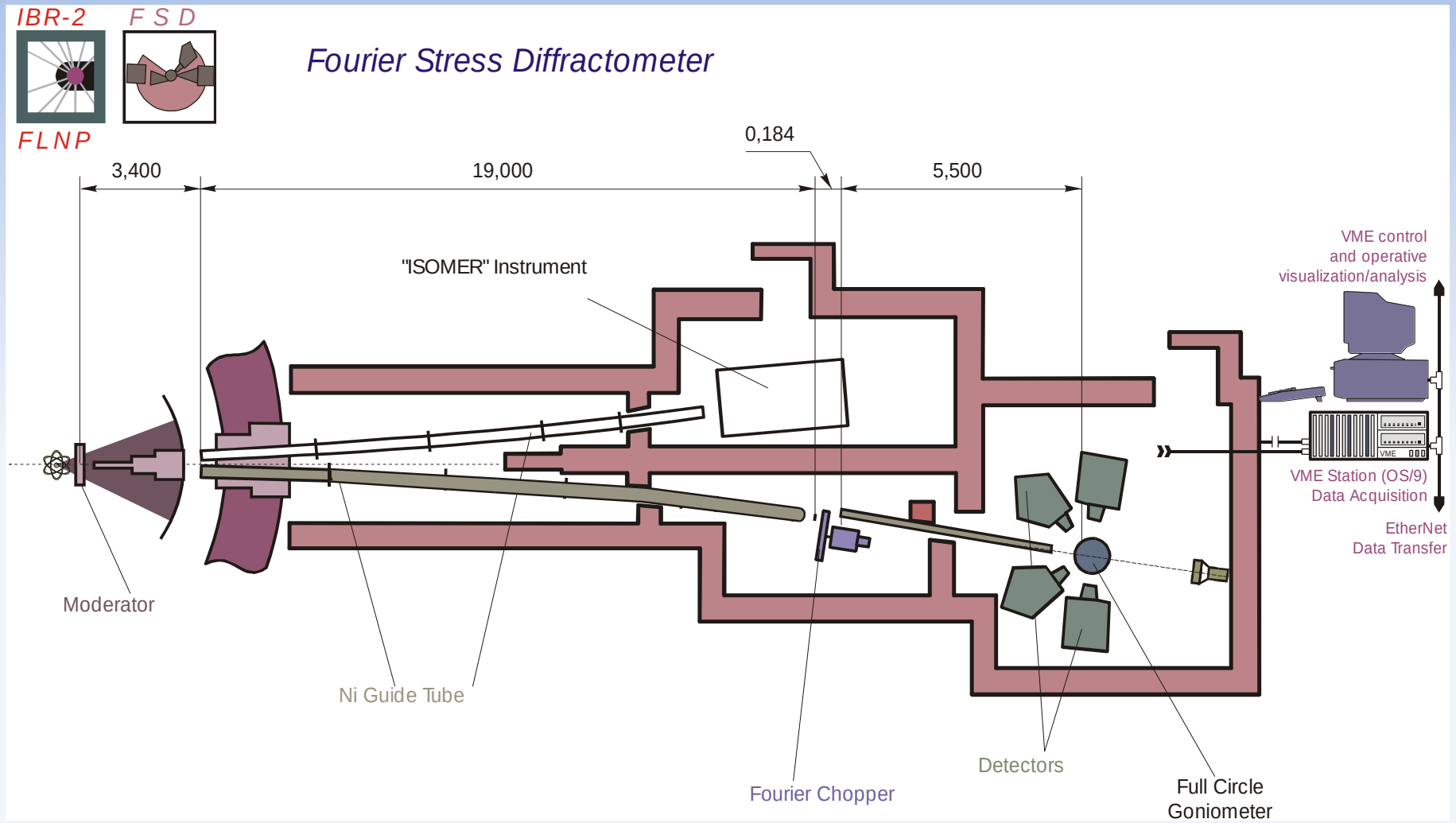

FSD diffractometer

90º-detectors

Backscattering detector

Fourier chopper

Sample position

Neutron guide

FSD: list of performed works

May 2012	Replacement of F-chopper control unit VectorDrive due to frequent failures
June 2012	Webcam for sample control Remote control of experiment (RDP protocol)
Sept. 2012	New ^{6}Li detector for neutron transmission experiments in high-resolution mode
June 2013	New 4-axis **Huber goniometer** (up to 300 kg)
April 2014	Replacement: new optical incremental encoder on F-chopper (instead of magnetic one)
Nov. 2014	New **AstraLeft4** detector module New **list-mode DAQ unit** (MPD-32 module) 1st version of list-mode **algorithm lmRTOF** for high resolution spectra reconstruction
May 2015	Adaptation of **stress rig LM-29** (up to 29 kN) for uniaxial tension/compression of samples Stress rig LM-29: **combination stress + high temperature**
Dec. 2015	New **AstraRight4** detector module New alignment linear lasers with remote control (Arduino)
March 2016	New **wide-aperture radial collimators** (JJ-Xray, Denmark) Replacement: temperature controller Lakeshore Model 325 for mirror furnace
Sept. 2016	Replacement: new control PC with Win7 OS and SONIX+ diffractometer control system
Oct. 2016	Possibility of remote reset of NIM crate with LM-DAQ unit (Arduino)
Oct. 2016	Replacement: new high-voltage supplies for BS and AL/AR detectors (iSeg GmbH) New 2-Circle Segment ±15° (Huber GmbH)
May 2017	**BS detector: separate signal acquisition** from individual PMTs (E-focusing)
May 2017	LM-DAQ: software adjustment of input signal parameters (dead time, signal duration and threshold levels)
Oct. 2017	Upgrade of **lmRTOF algorithm**: version for multi-detector systems
May 2018	New incident beam diaphragm (JJ-Xray)
June 2018	New load cell U10M (Fmax=125 kN) for stress rig LM-29 (HBM GmbH)
Sept. 2018	Electric lighting improvement Vacuum leak elimination in the neutron guide
Nov. 2018	Replacement: reactor starts distribution unit
Jan. 2019	**Cooling system for MF-2000** mirror furnace - Lauda UC4 chiller
2019	**Complete installation of ±90° detectors banks** (by Spectrometers Complex Dept.)
Jan.'18 June'18 Aug.'18 Nov.'18 June'19 Aug.'19 Oct.'19	**New F-chopper:** + Signing of the contract (348 kEuro) + Kick-off meeting at Airbus (Germany) + Preliminary Design Review (PDR) + Final Design Review (FDR) – End of Manufacturing and assembly – Factory Acceptance Test (FAT) – Installation + onsite commissioning at JINR

FSD detector system

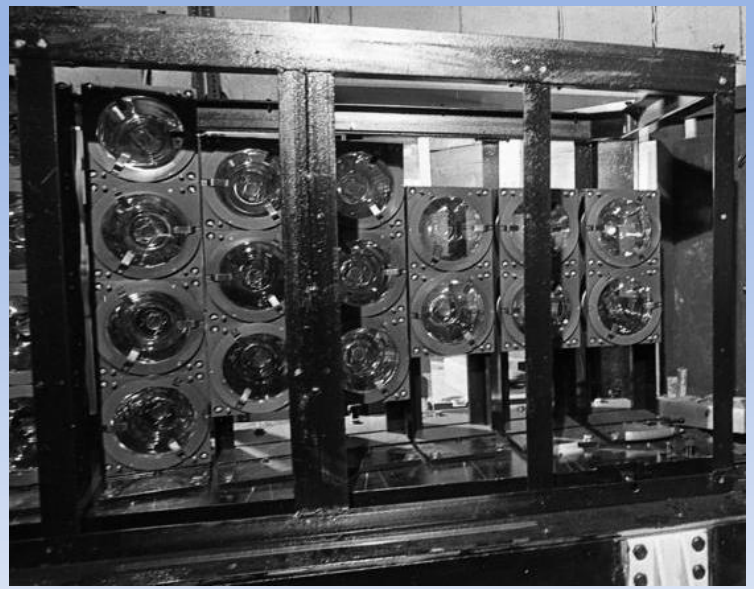

^{6}Li glass backscattering detector, 16 PMTs, resolution $\Delta d/d \approx 2 \times 10^{-3}$

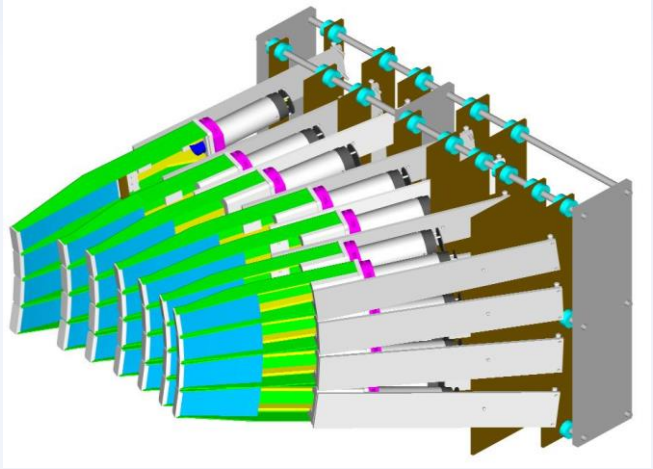

90º-detector bank: ZnS(Ag) scintillator with WLS-fibers

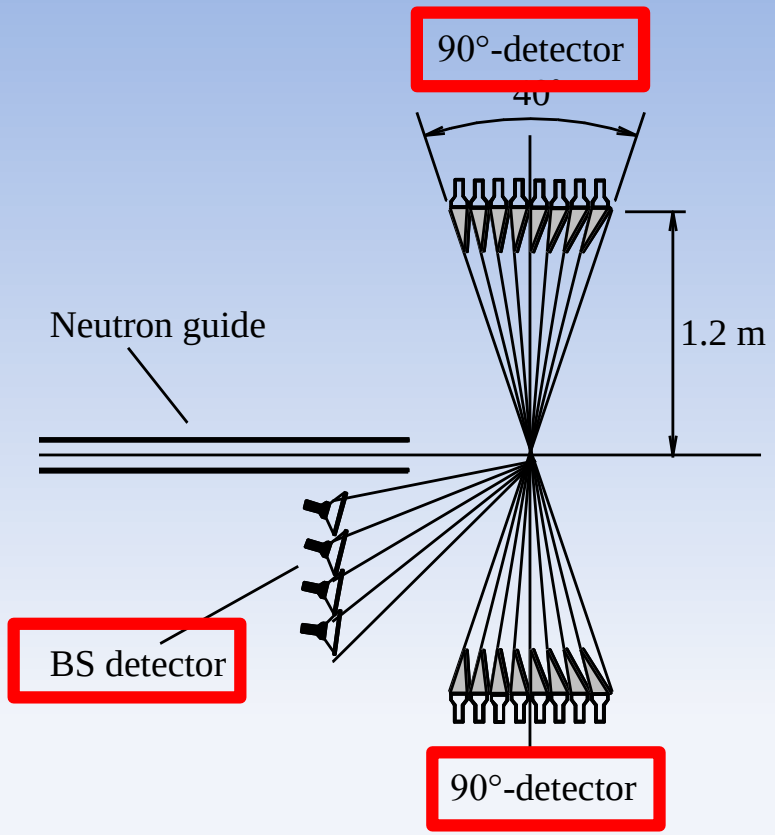

Interior arrangement of the single module

Scattering angle range $\Delta(2\theta) = \pm 20°$, azimuthal angle range $\Delta\varphi = 24°$, total solid angle $\Delta\Omega = 0.117$ str, resolution $\Delta d/d \approx 4 \times 10^{-3}$

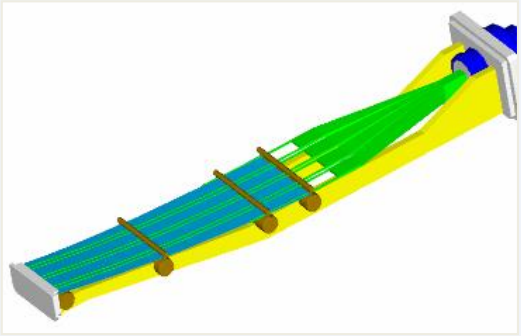

Upgrade of ±90° ASTRA detectors

AstraLeft-4: Nov. 2014

AstraRight-4: Dec. 2015

Task for 2019: complete installation of AL and AR detector banks (by Spectrometers Complex Dept.)

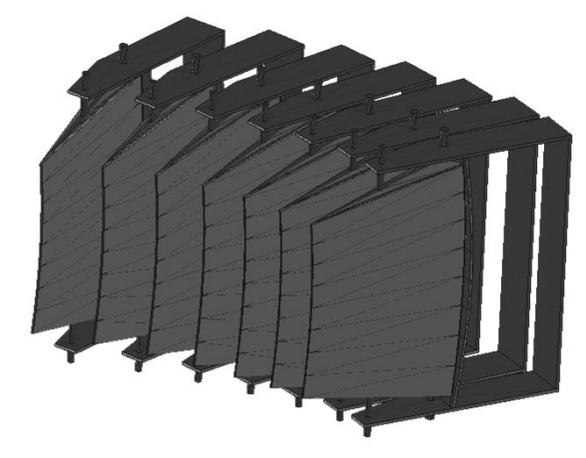

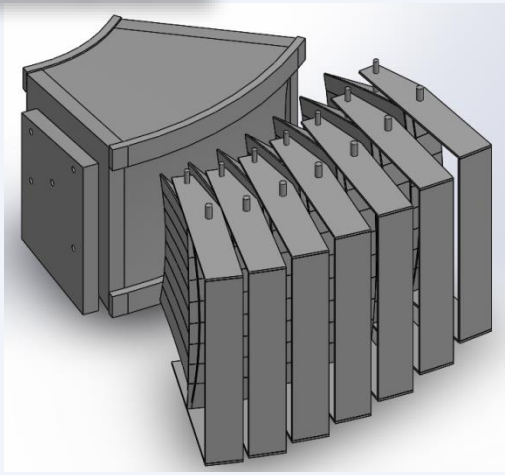

Sample positioning

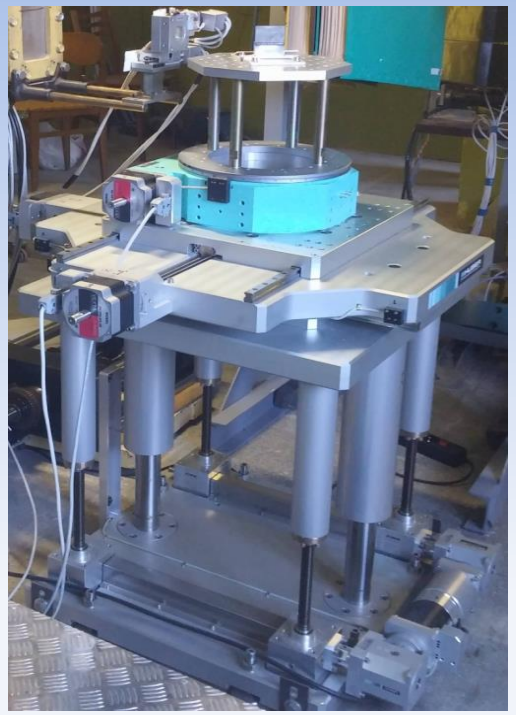

2013: 4-axis HUBER goniometer

Linear: X, Y: ± 150 mm

Linear: Z: 0 ÷ 300 mm

Rotation: Ω: 0 ÷ 360°

Max. load: 300 kg

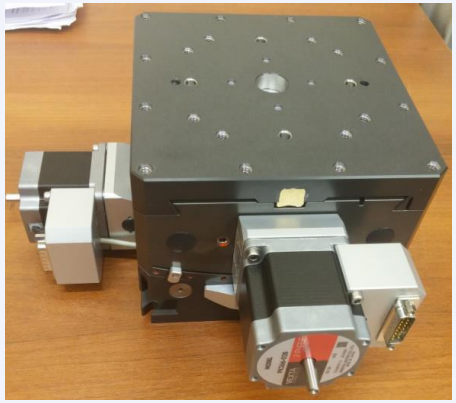

2016: 2-Circle Segment ±15° (Huber)

2016: New wide-aperture radial collimators (G.V.=1.8 mm)

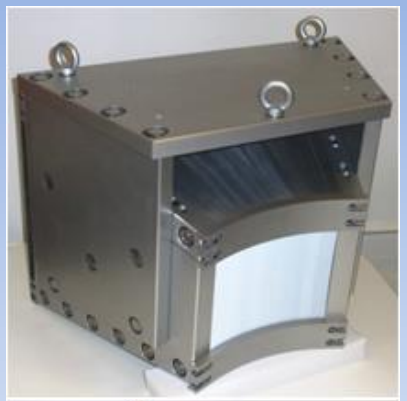

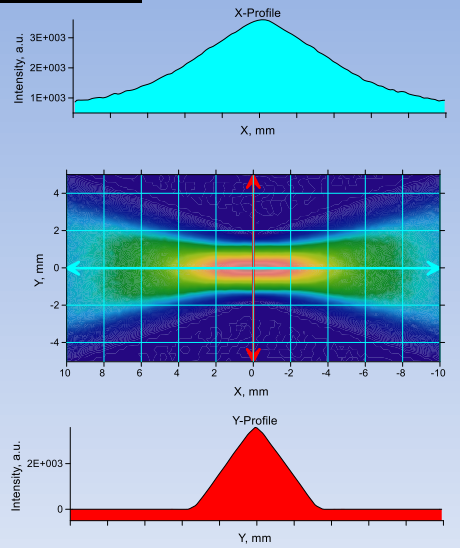

Beam profiles: analytical calculations and Monte Carlo simulation

Radial collimators on FSD for gauge volume definition in bulk sample during stress measurements

Two radial collimators by JJ X-Ray (Denmark)

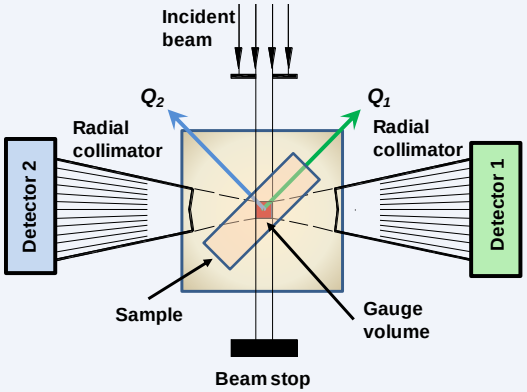

Strain measurement in bulk specimen with radial collimators

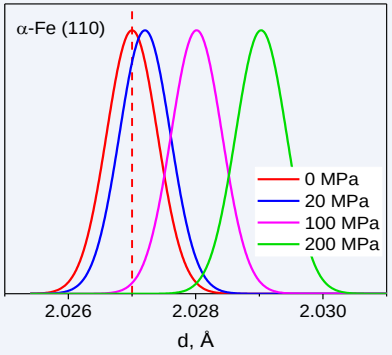

Diffraction peak shift at different stress values

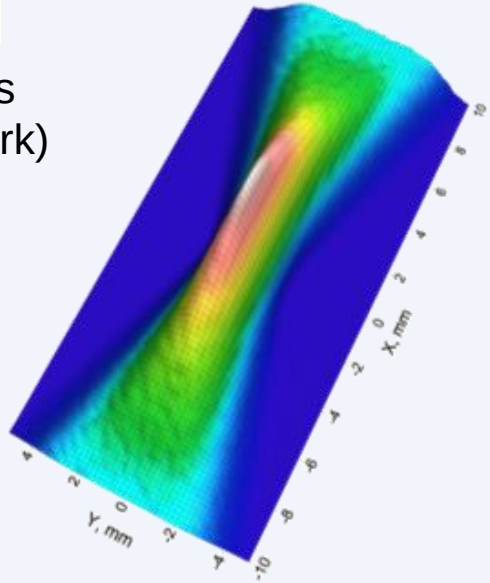

New wide-aperture radial collimators (G.V.=1.8 mm)

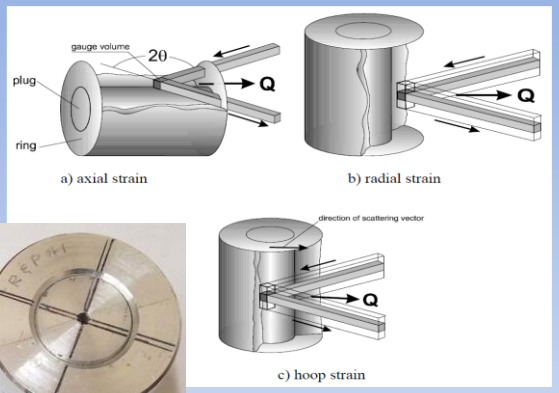

Collimators **can be removed** from the beam using specially designed movable platform

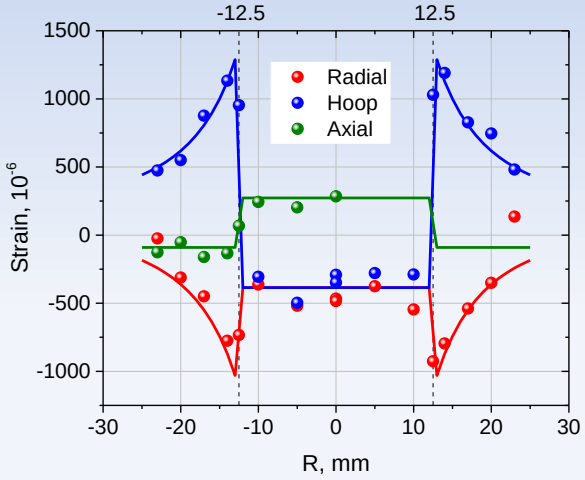

Max. penetration depth ~27 mm

Scattered beam profile scan with Ø1 mm sample

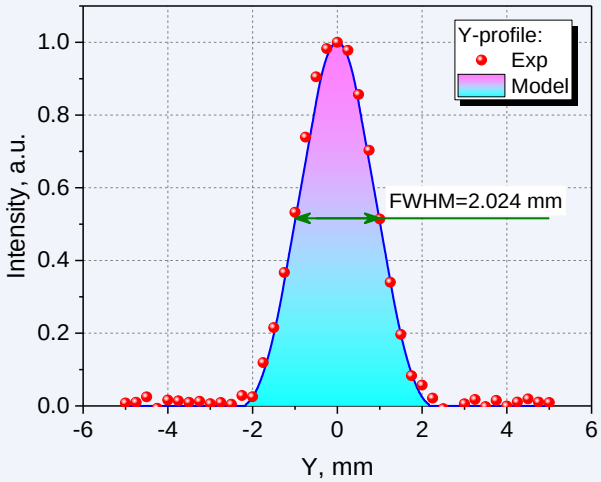

Flat steel plate surface position determination by G.V. scan

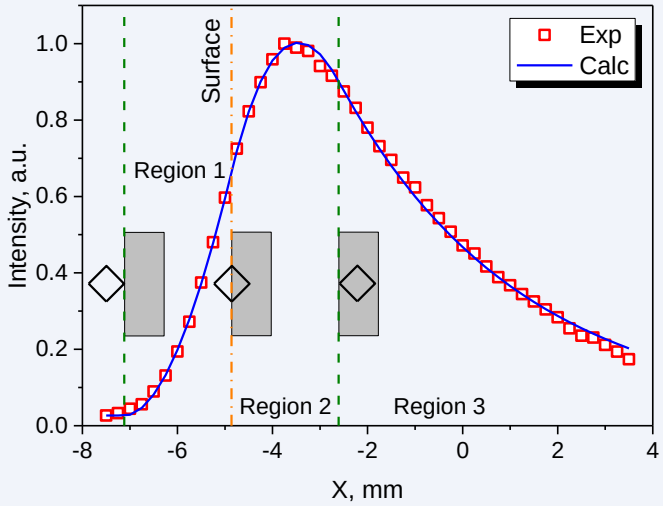

Residual lattice strain measured in standard VAMAS sample (shrink-fit ring and plug, set #1)

Multi-pass welded specimen: FEM and neutron diffraction

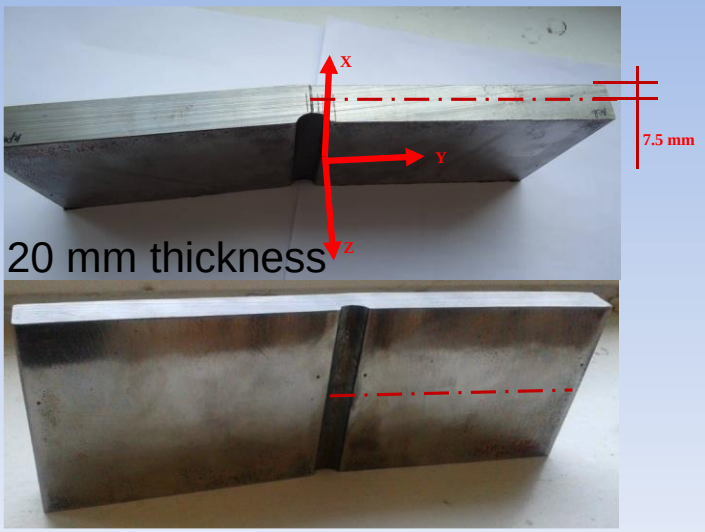

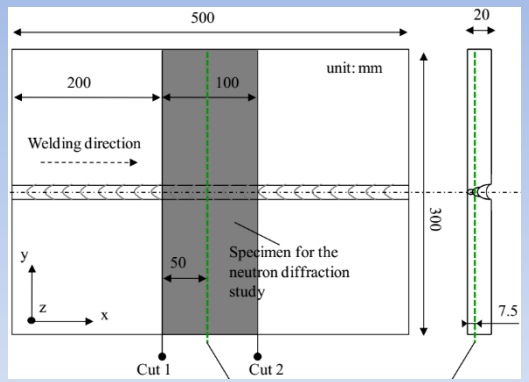

Specimen for the neutron diffraction study prepared by cutting from the entire multi-pass welded joint and position of the path "S" for the measurement of residual welding stresses

Multi-pass welded test specimen (300x100x20 mm)
-1st weld pass: MSG (Metal Active Gas welding)
-2nd and 3rd weld passes: SAW (Submerged Arc Welding)

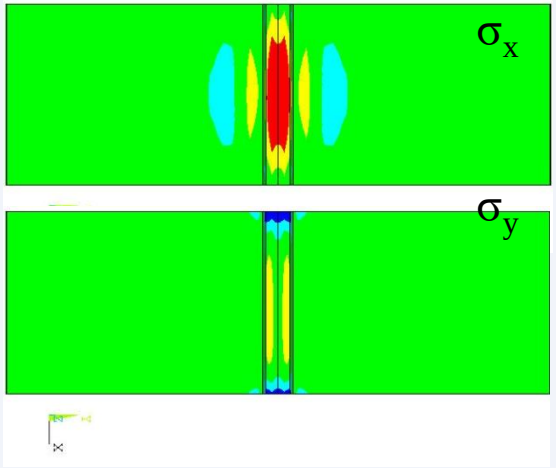

FEM results for longitudinal σ_x and transversal σ_y stress

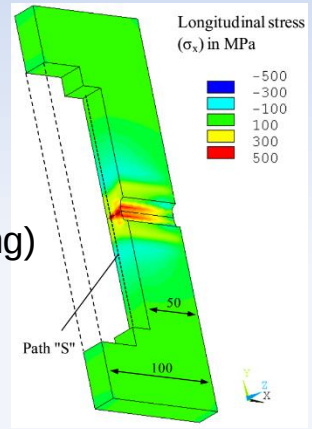

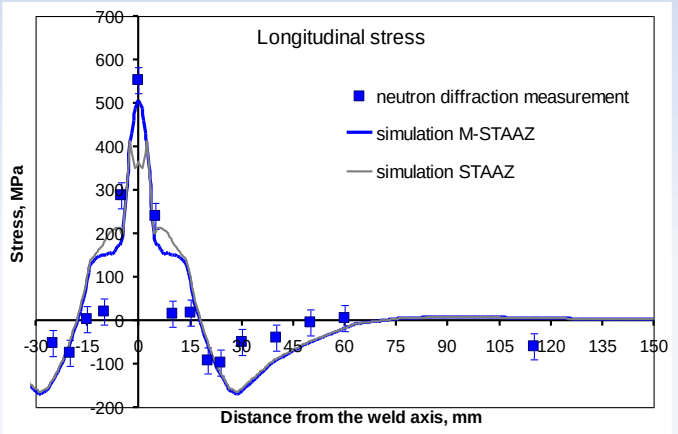

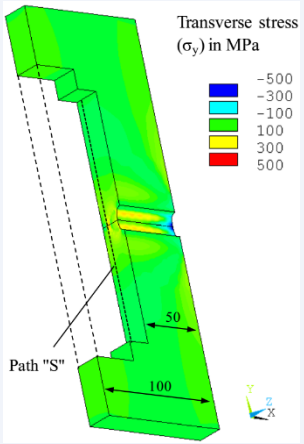

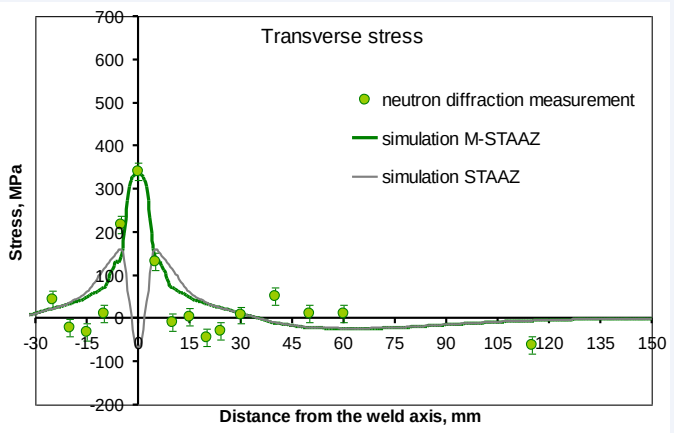

G. Genchev, G. Bokuchava, P. Petrov et al., J. of Constructional Steel Research, 2017, V. 138, pp. 633–641.

Charpy surveillance specimens reconstituted by electron and laser beams

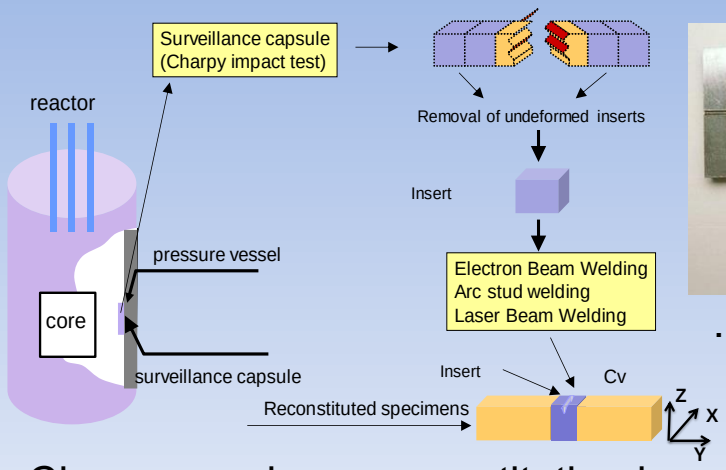

Charpy specimen reconstitution by…

… arc stud welding (ASW)

in collaboration with Institute of Electronics of BAN (Sofia, Bulgaria)

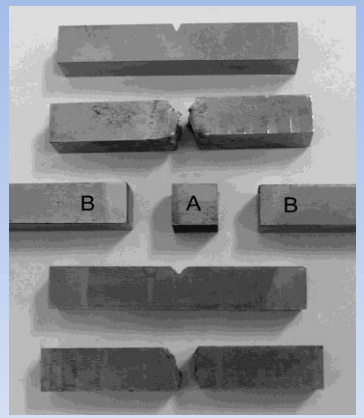

… electron (EBW) or laser (LBW) beam welding

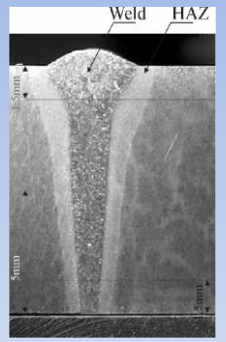

Typical macrostructure of weld joint

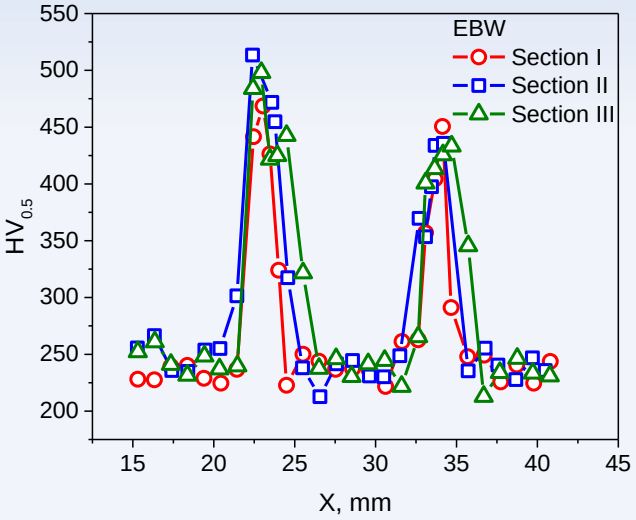

Microhardness distribution for EBW Charpy specimen

Specimens studied by neutron diffraction

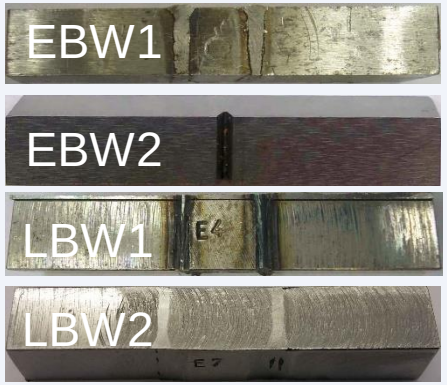

DBTT shift ?

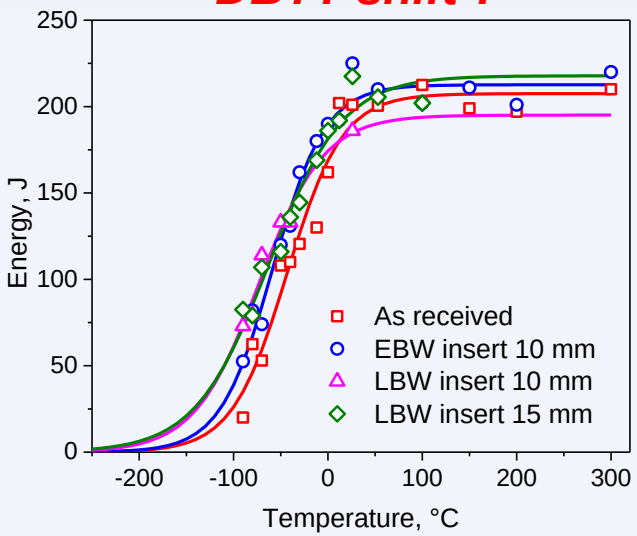

Total absorbed energy during Charpy impact tests

G.D. Bokuchava, P. Petrov et al., J. of Surface Investigation. X-ray, Synch. and Neutr.Techn., 2016, Vol.10, Issue 6, pp. 1143-1153

Charpy surveillance specimens…

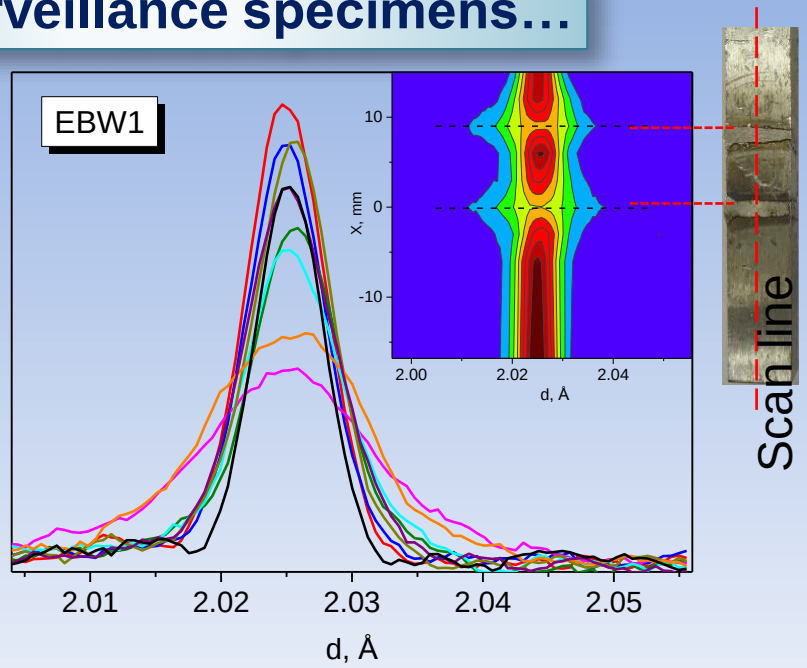

Diffraction peak (110) shape changes during scan across weld seams for EBW1 specimen. Inset: intensity map

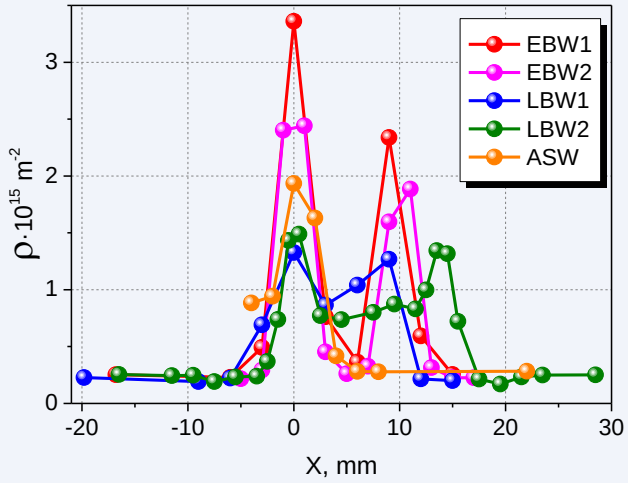

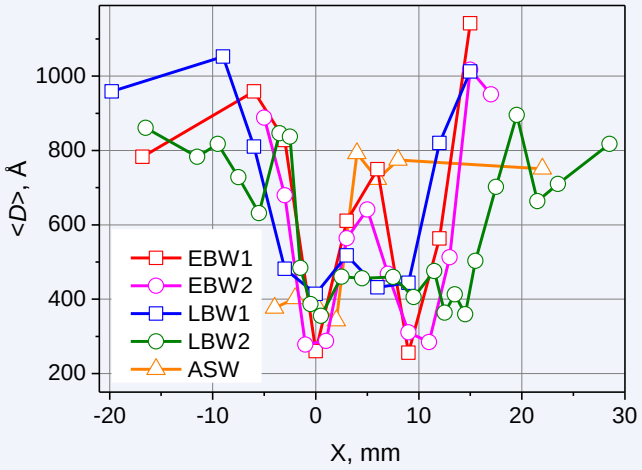

Dislocation density (**left**) and crystallite size (**right**) distributions for Charpy specimens. Weld seam centers - at X = 0 mm and X = 9 mm (X=14 mm for LBW2)

Residual stress distribution

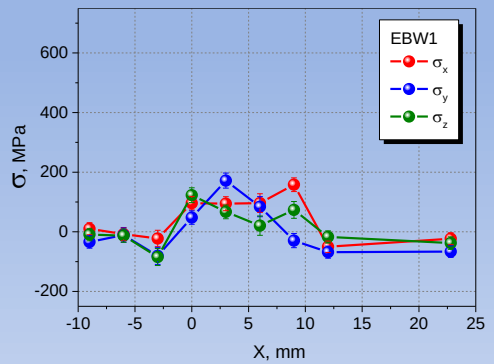

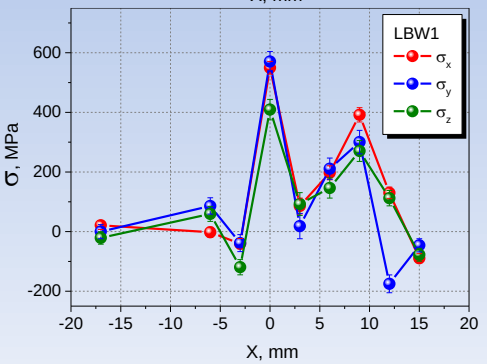

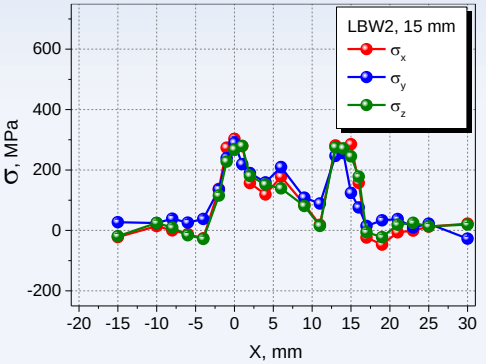

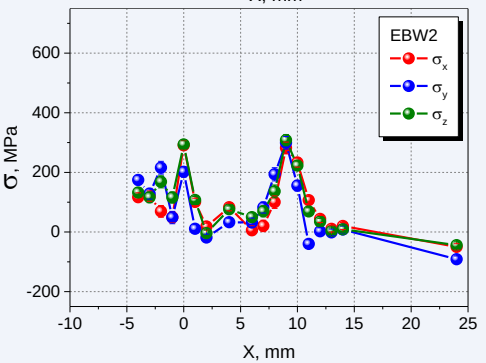

Mirror furnace MF-2000 for experiments at elevated temperatures

power - 1 kW
max. temp. - 1000° C
Temperature control by LakeShore 325

2019: chiller Lauda UC4

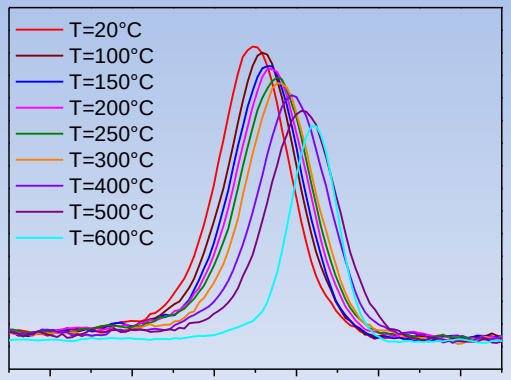

Diffraction peak (211) position and shape vs. temperature.

Dispersion-hardened ferrite-martensite steel

Studied sample in mirror furnace

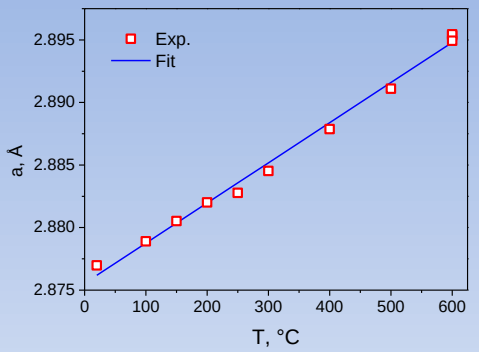

Lattice parameter changes vs. annealing temperature

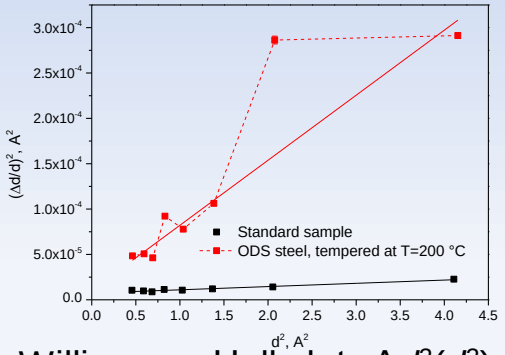

Williamson-Hall plots $\Delta d^2(d^2)$

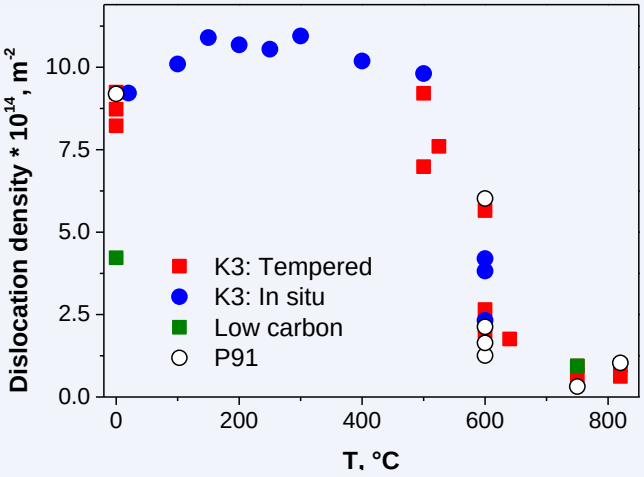

Dislocation density vs. annealing temperature

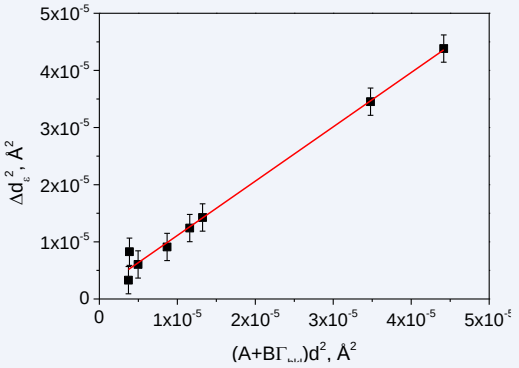

Squared peak width Δd^2 vs. $(A+ BH^2)d^2$ at T=200°C

G.D. Bokuchava, Rom. J. of Physics, 2016, Vol. 61, No. 5-6, pp. 903-925.

2015: Stress rig LM-29

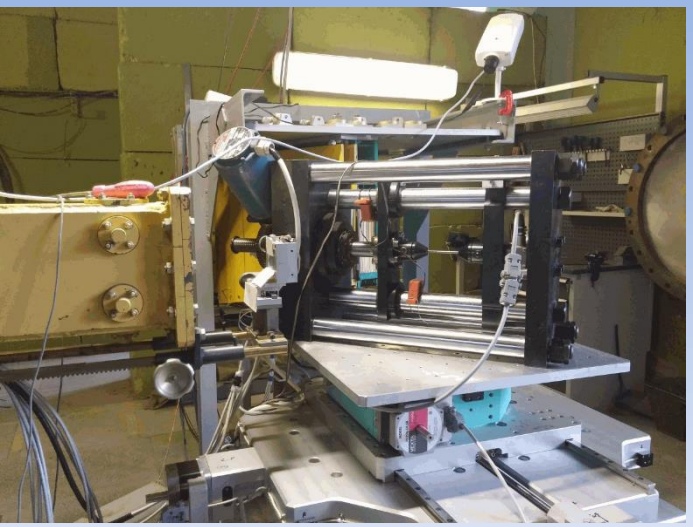

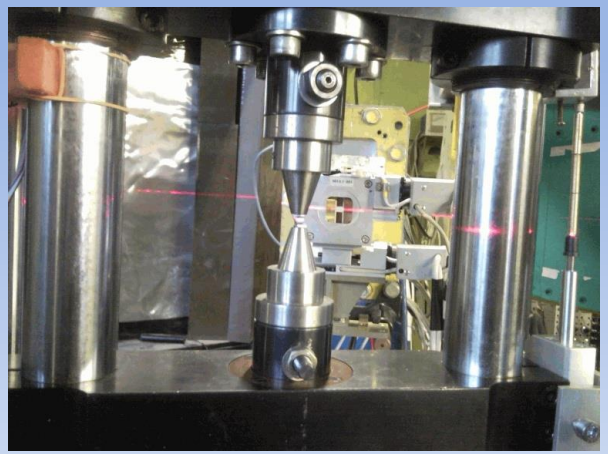

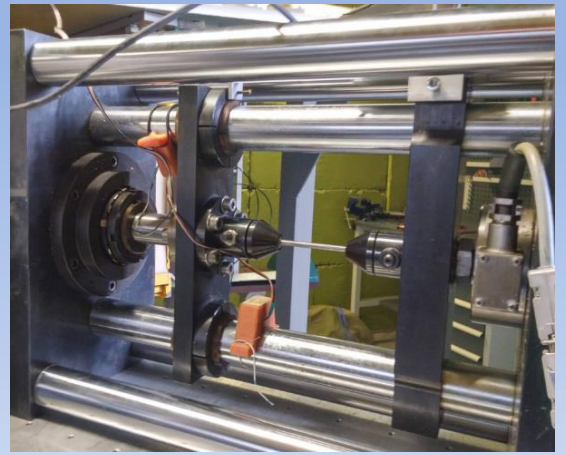

Uniaxial mechanical stress rig LM-29 (F_{max} = ±29 kN, T_{max} = 800°C). Controlled by PC (OS WinXP). Integrated into FSD control system using Pascal and Python scripts

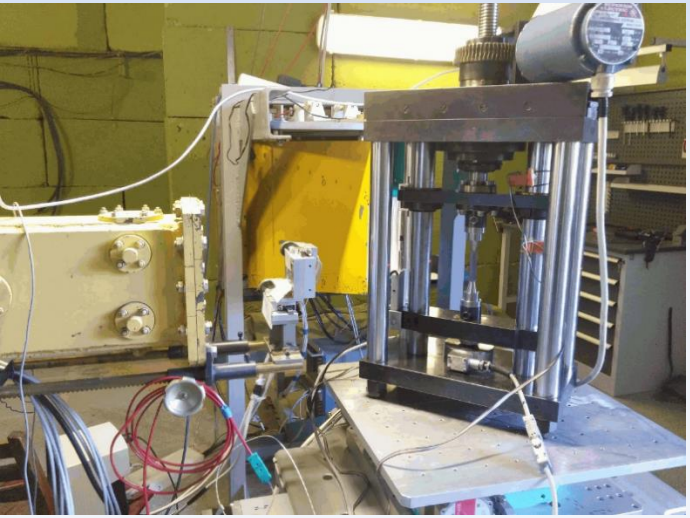

Stress rig LM-20 can be installed horizontally or vertically

Grips for flat samples

Grips for tests at **room** and **elevated** temperatures with M10, M12, M14 screws

Conical grips (with holders) for **<u>compressive tests</u>**

Austenitic steel: applied load/cycling

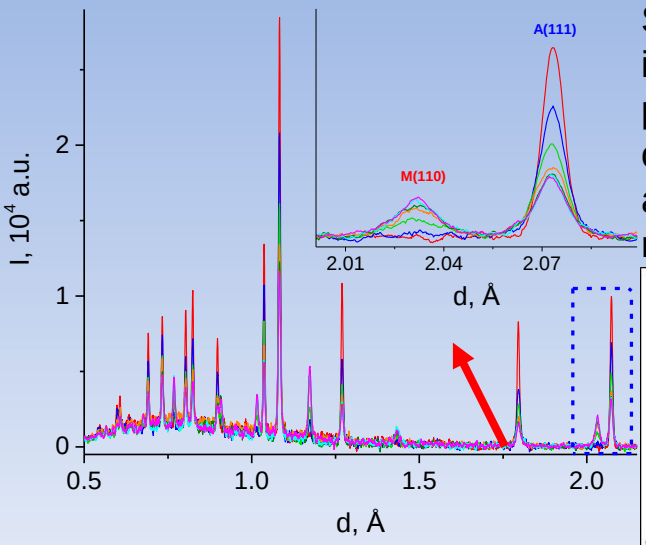

Spectra from austenitic steel: initial and after cycling with plastic deformation. Inset: part of neutron spectra with (111) austenite and (110) martensite reflections.

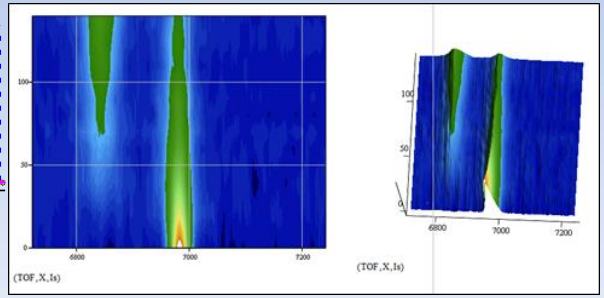

3D intensity map evolution vs. applied load

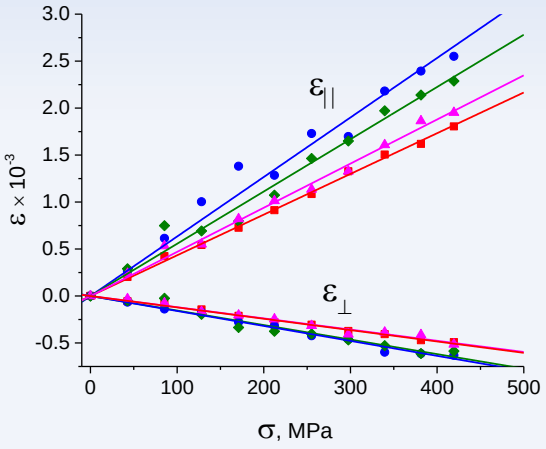

Anisotropic lattice strain for different reflections (hkl) vs. applied load.

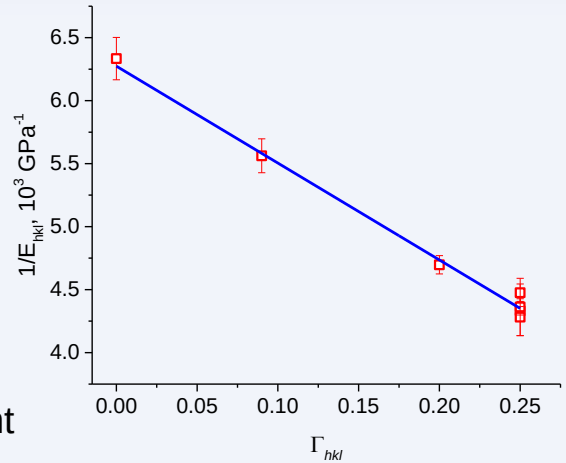

Inverse Young's modulus vs. anisotropy factor Γ_{hkl}

Aluminum alloy D16: applied load + temperature

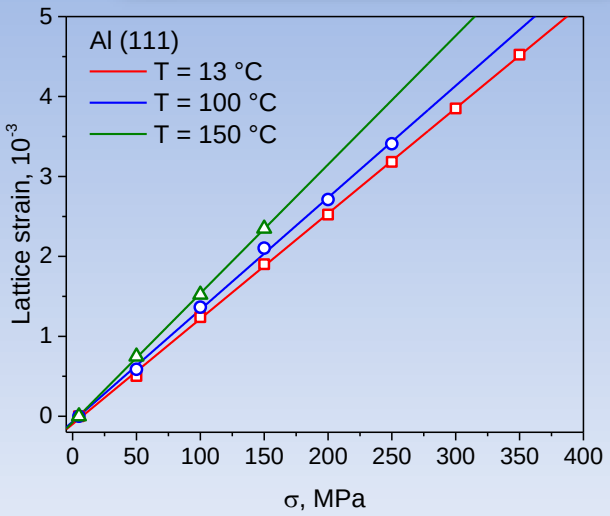

Lattice strain for Al (111) peak vs. applied load at different temperatures

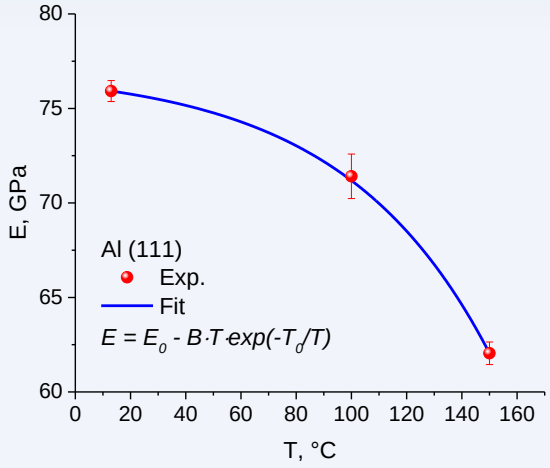

Young's modulus vs. temperature

G.D. Bokuchava, I.V. Papushkin, J X-ray, Synch. and Neutr.Techn., 2018, Vol. 2, pp. 5-11.

TRIP steel

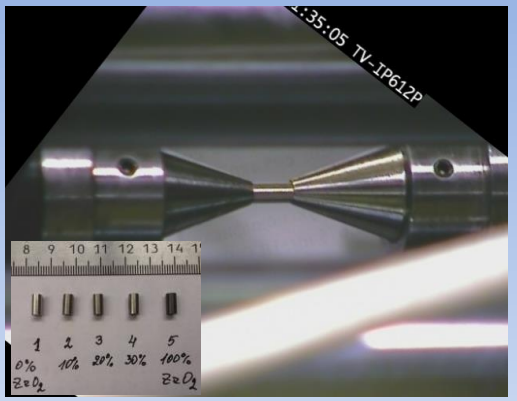

Sample in stress rig

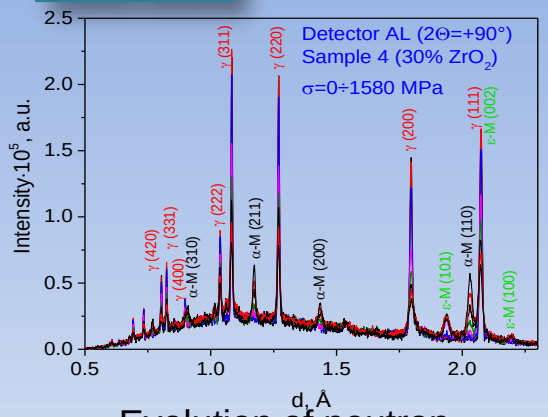

Evolution of neutron diffraction pattern

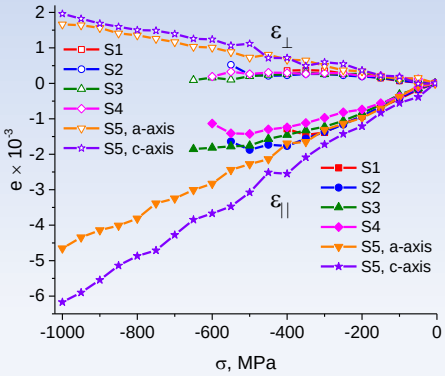

Austenite matrix lattice strain

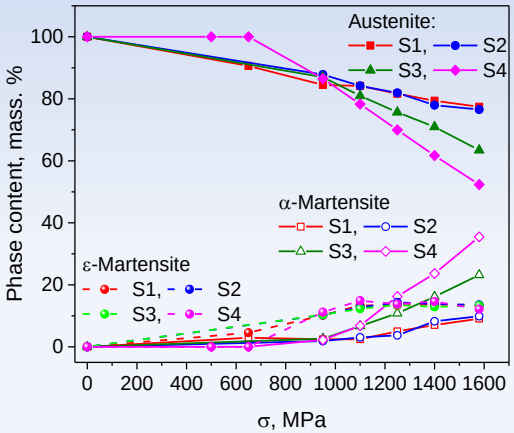

Phase contents vs. plastic deformation

4 phases:
Austenite (matrix), ZrO_2, α- and ε-martensite

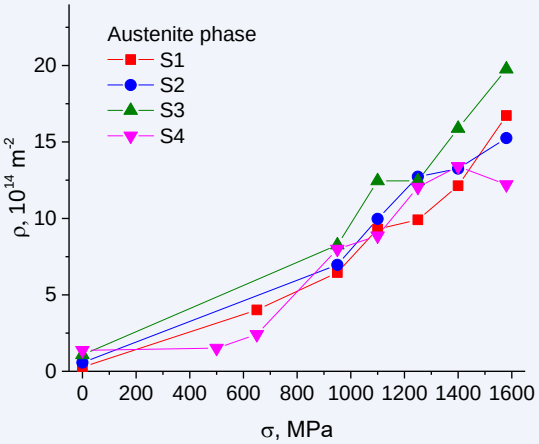

Dislocation density for austenite matrix vs. plastic deformation

W/Cu composites

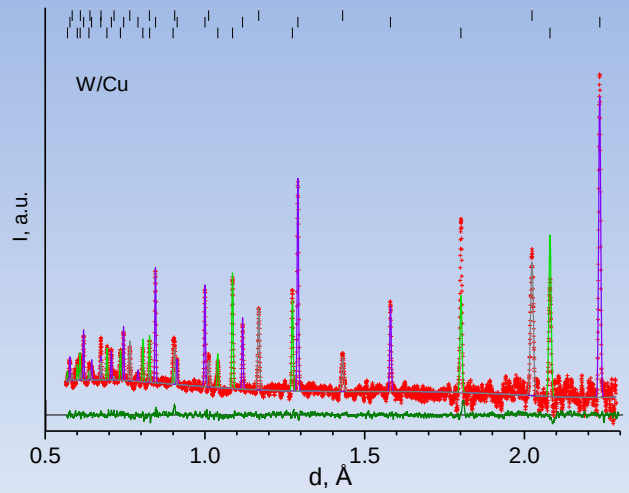

Neutron diffraction spectrum from W/Cu composite processed by Rietveld method

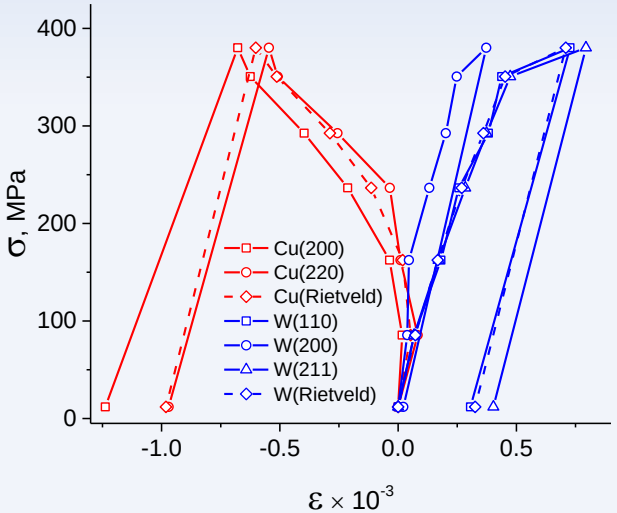

Lattice strain for Cu and W phases of W/Cu composite vs. applied load

G. Bokuchava, Crystals, 2018, Vol. 8, Issue 8:318

List-mode DAQ unit development:

1997: First ideas - V.A. Kudryashev, V.A. Trounov, V.G. Mouratov, Physica B, 1997, Vol. 234-236, pp. 1138-1140.

2012: Development of the new list-mode DAQ unit (FLNP JINR, Dubna)

S.M. Murashkevich, F.V. Levchanovskiy, Proc. of the NEC'2013, Sept. 9-16, 2013, Varna, Bulgaria. JINR E10,11-2013-136, Dubna, 2013, pp.176-180.

Since 2014: Regular use on FSD, FSS and HRFD Fourier diffractometers

New list-mode DAQ unit - MPD (Multi Point Detector):

- based on five ALTERA FPGAs
- number of detector signals - up to **240**
- sampling frequency - 62.5 MHz, i.e. discretization time - **16 ns**
- max. exposition time = $4.5 \cdot 10^6$ sec.=**1250 hours**=52 days (defined by time counter capacity - 48 bits)
- data transfer between MPD and control PC - by 1.25 Gbit/s fiber optics network and USB 2.0
- two operation modes:
  - **histogram**: low resolution TOF-spectra are accumulated in internal memory (64 Mb)
  - **list-mode**: raw data are recorded as 32-bit words (timestamps) with max. data flow rate of $8 \cdot 10^6$ events/sec.
- list-mode events are recorded in **absolute time of experiment**

On FSD the **MPD-32** DAQ unit with 32 input detector signals is installed for routine operation: detector events, reactor pulses and rising and falling fronts of Fourier chopper pickup signals.

NB: for Ωmax = 6000 rpm and exposition time T = 1 hour the typical raw data file size is of **900 Mb**, **~97%** of events are **pickup** signals. During a typical 11-day cycle of the IBR-2 reactor operation **150-200 Gb** of raw data is usually collected on FSD.

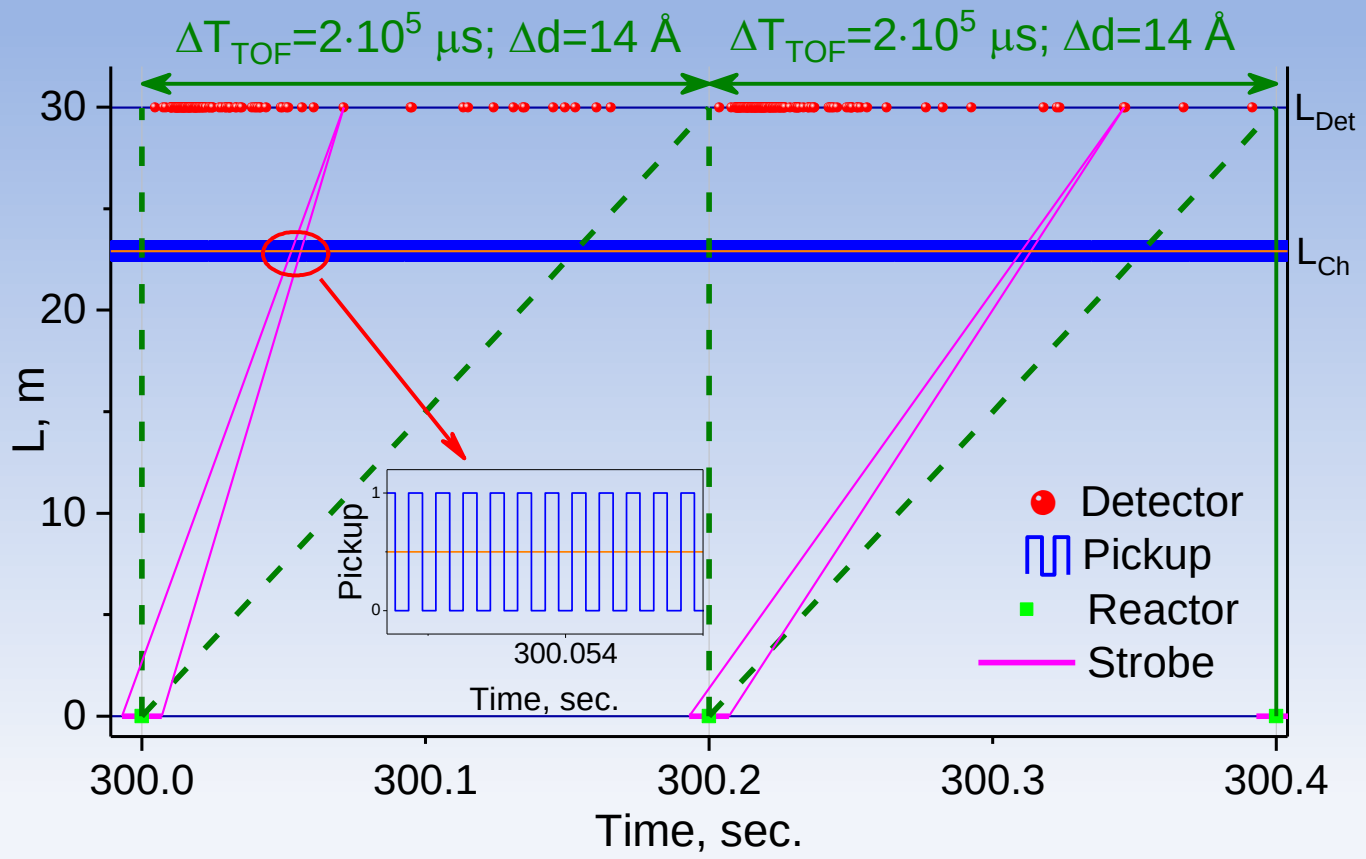

Timecode, ticks	Signal	Event
45080023003	240	Reactor start
45080024869	242	Pickup ↑
45080026730	29	Detector 29
45080028597	243	Pickup ↓
45080030461	5	Detector 5
45080034180	242	Pickup ↑
45080036045	16	Detector 16
45080037914	1	Detector 1
45080039776	243	Pickup ↓
45080041638	7	Detector 7
45080043504	242	Pickup ↑
45080045371	26	Detector 26
45080047238	17	Detector 17
45080049099	243	Pickup ↓
45080050979	4	Detector 4
45080052833	242	Pickup ↑
45080054701	22	Detector
45080056567	243	Pickup ↓
45080058436	31	Detector 31
45080060296	242	Pickup ↑

1 tick = 16 ns

Time diagram of the list-mode events for 2 reactor pulses. Recorded events: reactor pulses, chopper pickups and detector signals. Horizontal axis - absolute time of measurement, vertical axis - flight path (neutron source position at $L = 0$, Fourier chopper position at $L = L_{Ch}$ and detector position at $L = L_{Det}$). The whole TOF range between reactor pulses is about $2 \cdot 10^5$ μs, which corresponds to reactor repetition rate of 5 Hz. Reactor pulse occurred at the time point of ~300 μs ($L = 0$) and it is gated by strobe signal of the width W_S.

List-mode DAQ: high resolution spectra reconstruction from raw data

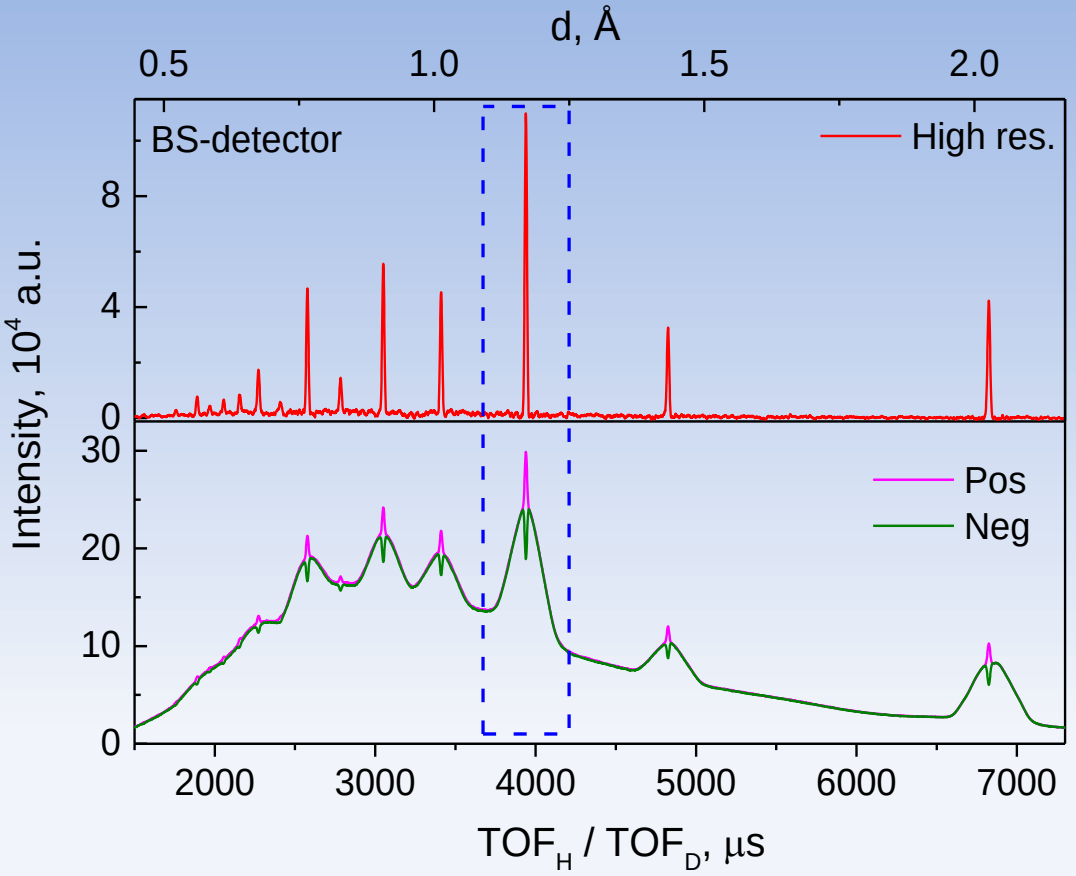

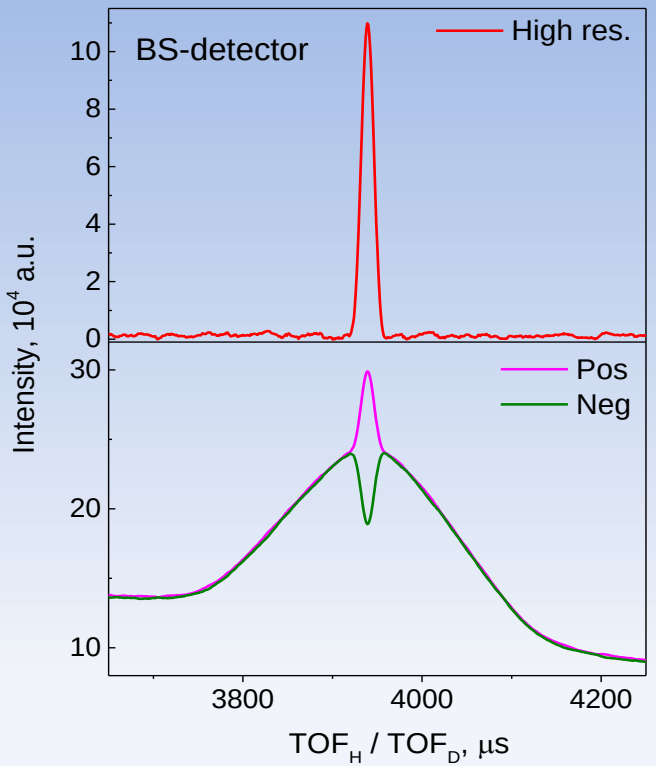

RTOF neutron diffraction spectra measured from standard α-Fe powder sample with the maximal Fourier chopper speed Ω_{max} = 4000 rpm. At the bottom "positive" $I^+(t)$ and "negative" $I^-(t)$ correlation spectra are shown. The upper pattern is high-resolution diffraction RTOF spectrum calculated as a difference of "positive" and "negative" patterns: $H(t) = I^+(t) - I^-(t)$.

Diffraction peak (211) region in the same RTOF spectra.

List-mode DAQ: comparison with old DAQ system

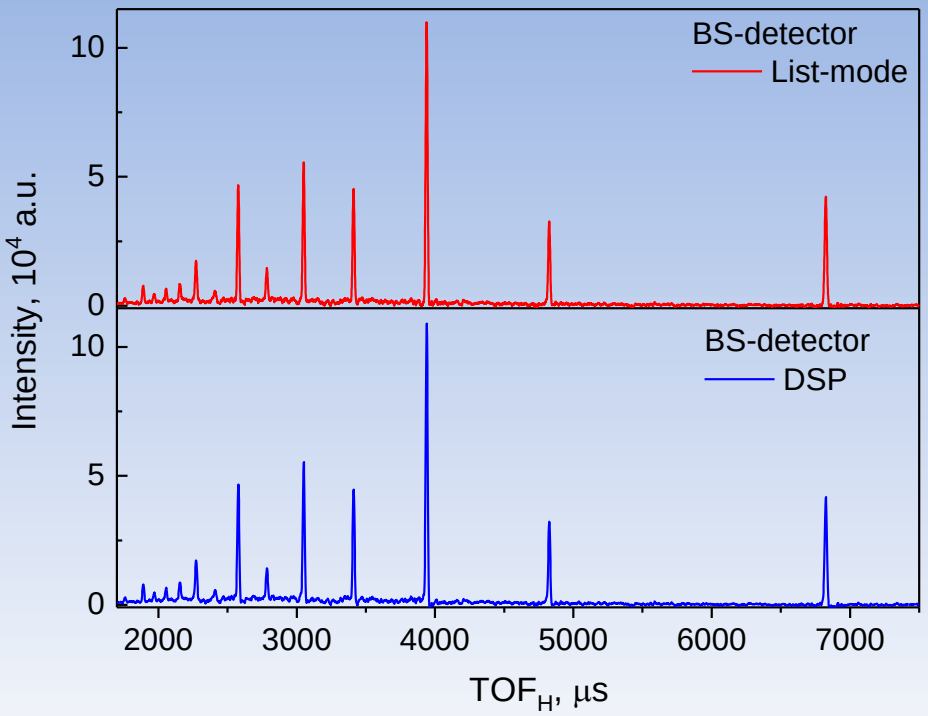

Old TOF parameters (DSP):
cw=2 mks, N_{chan}=3900 (limited!), d_{max} ~ 3 Å

New TOF parameters (LM MPD-32):
cw=1 mks, N_{chan}=20000 (up to 50000), d_{max} > 7 Å

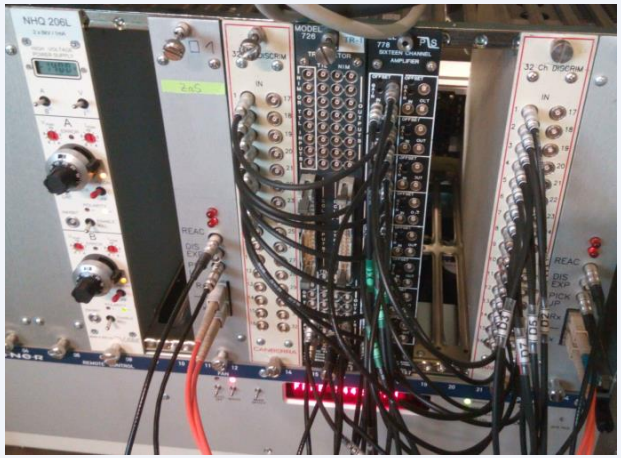

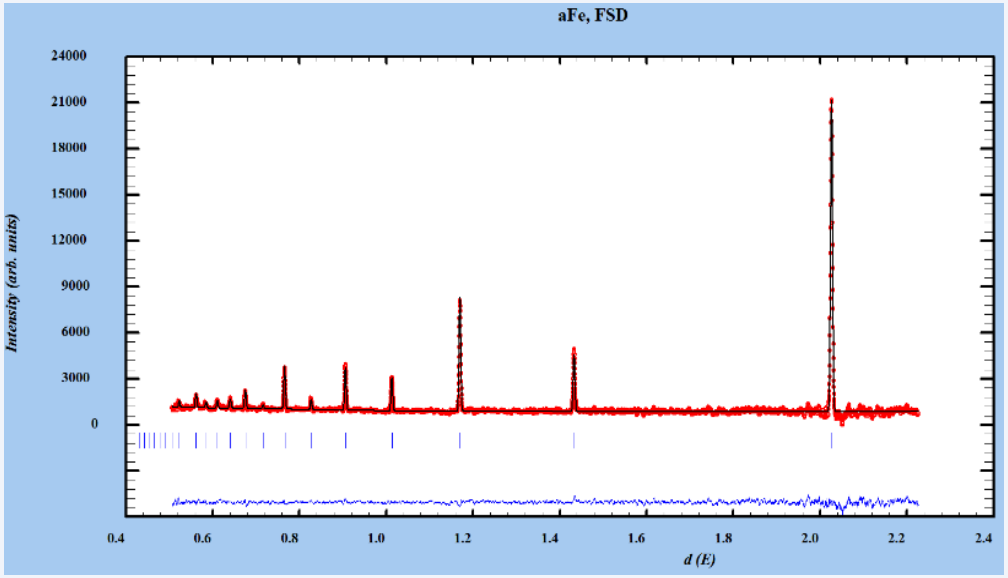

LM DAQ: Electronic focusing of detector modules

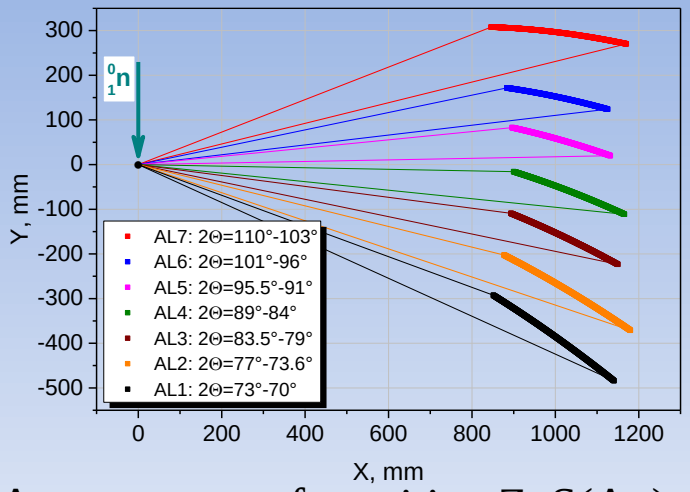

Arrangement of sensitive ZnS(Ag) layers of the ASTRA 90°-detector in the horizontal scattering plane

$$k_i = L_i \cdot \sin(\theta_i) / L_0 \cdot \sin(\theta_0)$$
$$\tau_i = k_i \, \tau_0$$

L_i, L_0 are the flight paths, θ_i, θ_0 are the scattering angles, and τ_i, τ_0 are RTOF channel widths for the *i*-th and basic detectors, respectively

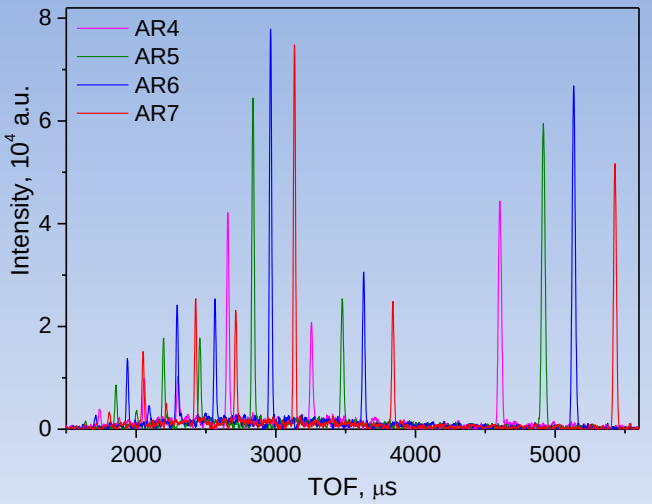

Initial diffraction spectra from individual modules of the ASTRA detector

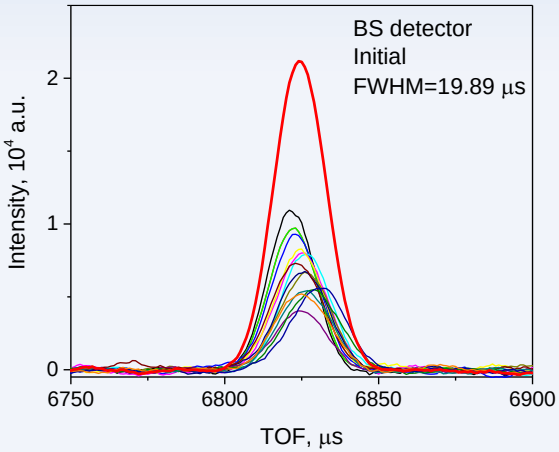

Initial spectra

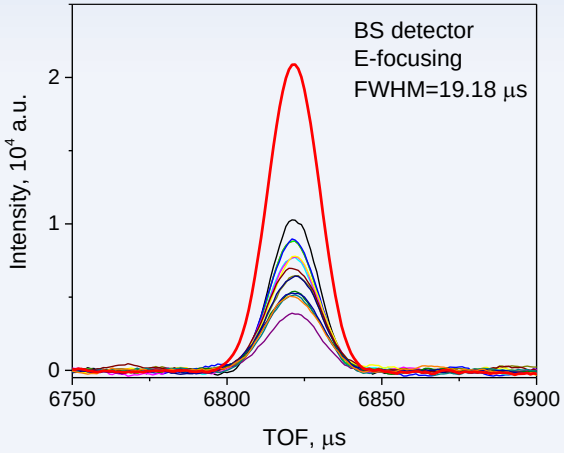

After E-focusing

Fine tuning of TOF-focused backscattering detector: additional E-focusing

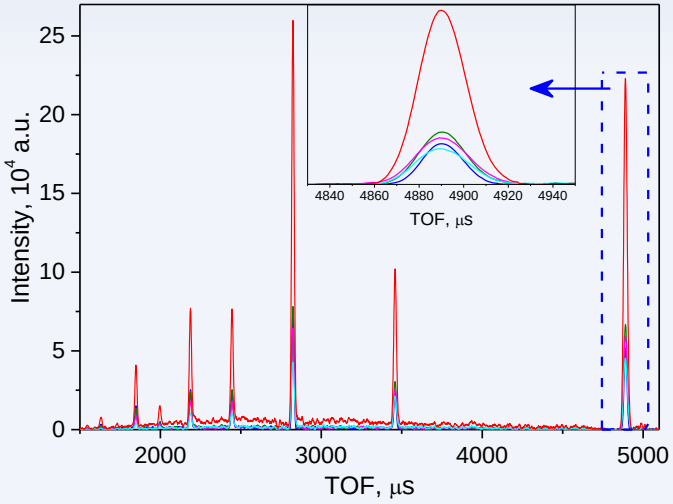

The same diffraction spectra reduced to the unified TOF scale (E-focusing) and the final total spectrum

LM DAQ: Phase error correction

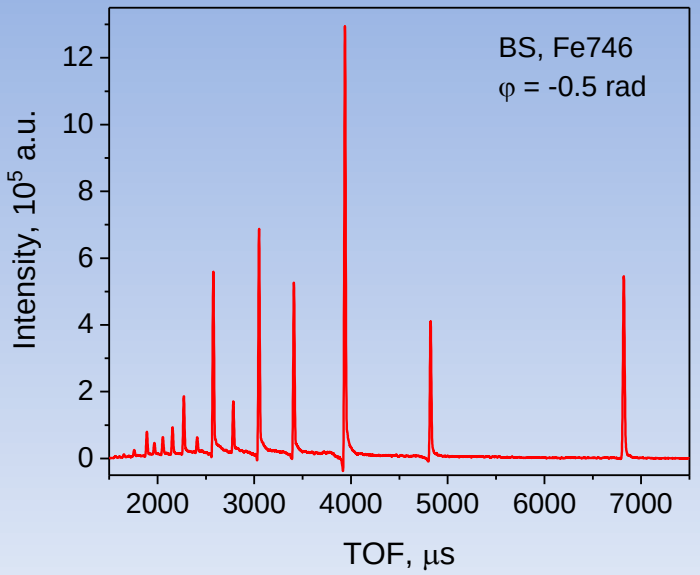

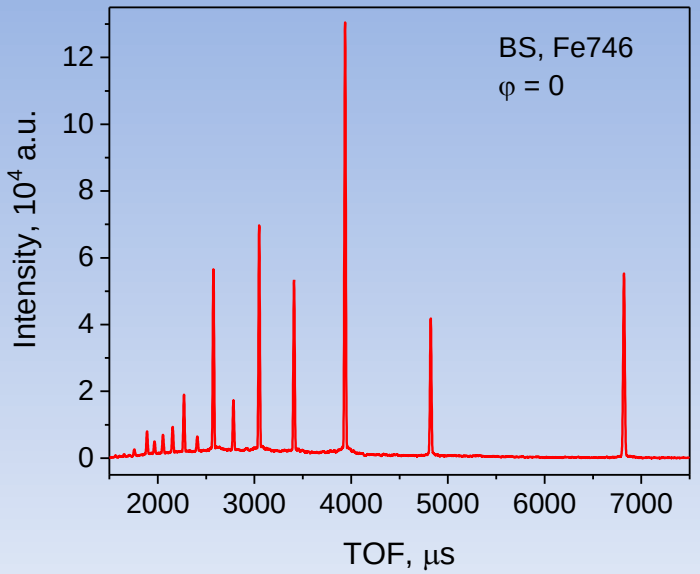

RTOF diffraction spectrum measured with -0.5 rad phase shift: initial (left) and corrected (right)

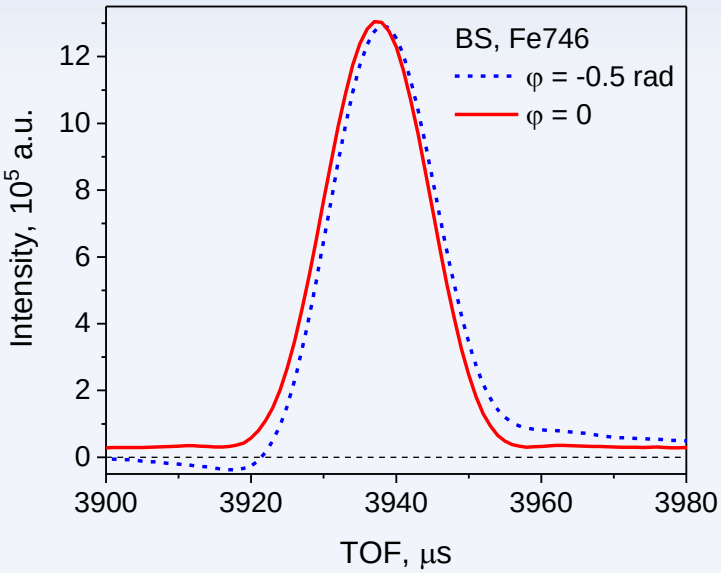

Diffraction peak profile after phase correction

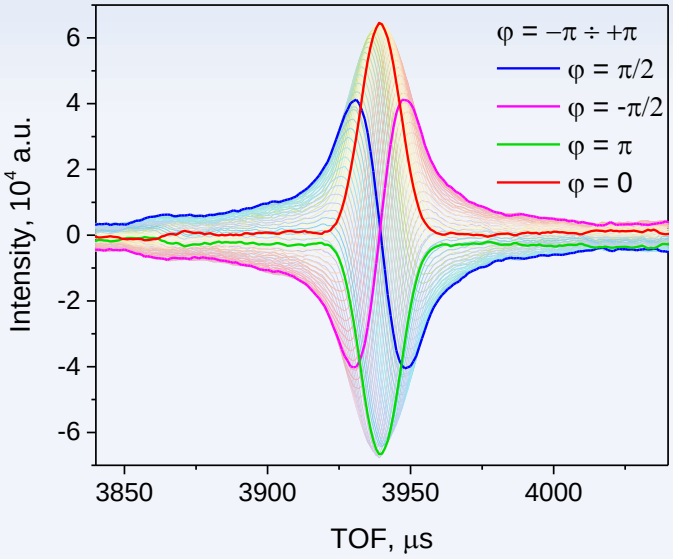

Set of experimental RTOF diffraction peak profiles reconstructed from raw data with phase parameter in the range $\varphi = -\pi \div \pi$

Real frequency window analysis: Dirichlet (linear) window

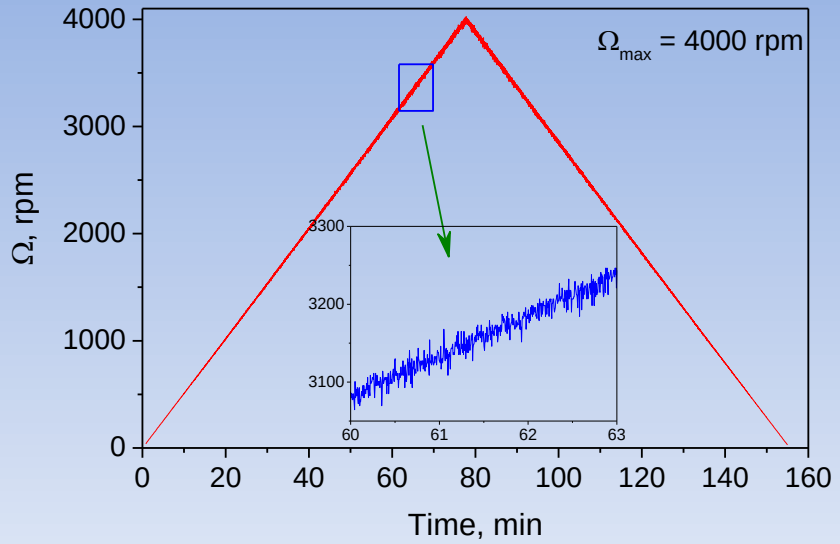

Dirichlet sweep function reconstructed from raw LM data. The inset shows the scatter of the optical encoder data.

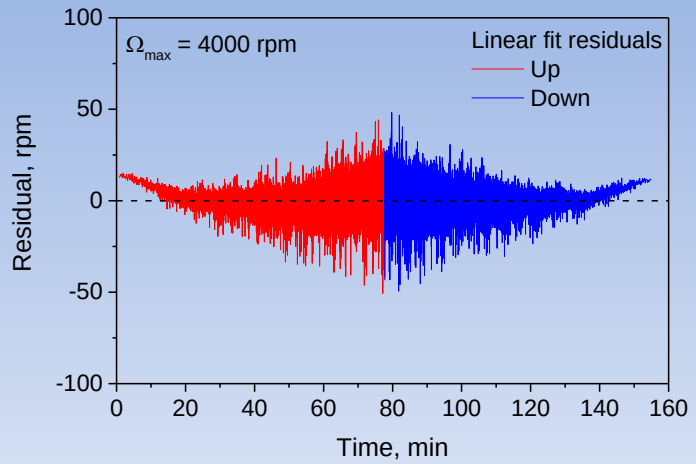

Linear fit residuals: deviations from linearity due to imperfect PID regulation.

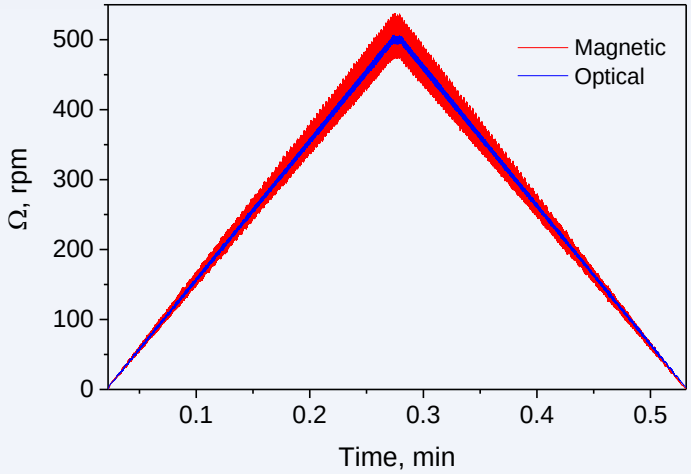

Comparison of Dirichlet sweep function measured with magnetic and optical encoders.

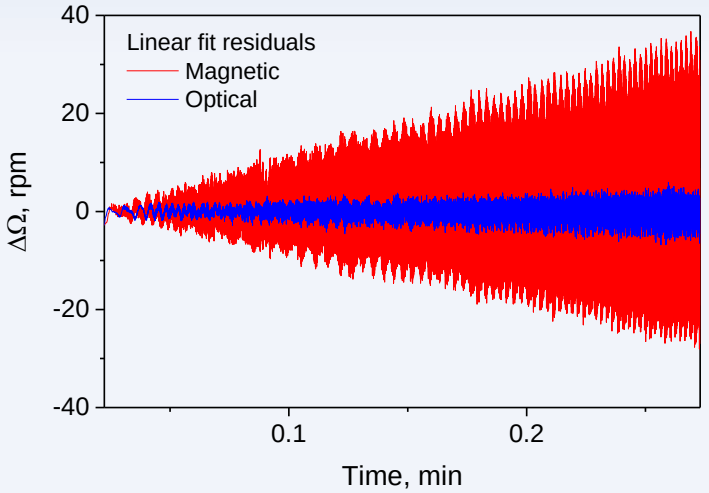

Comparison of corresponding linear fit residuals (pickup signal jitter) for magnetic and optical encoders.

LM DAQ: Real frequency window analysis - composite Blackman frequency windows (multiple Dirichlet sweeps with Blackman envelope)

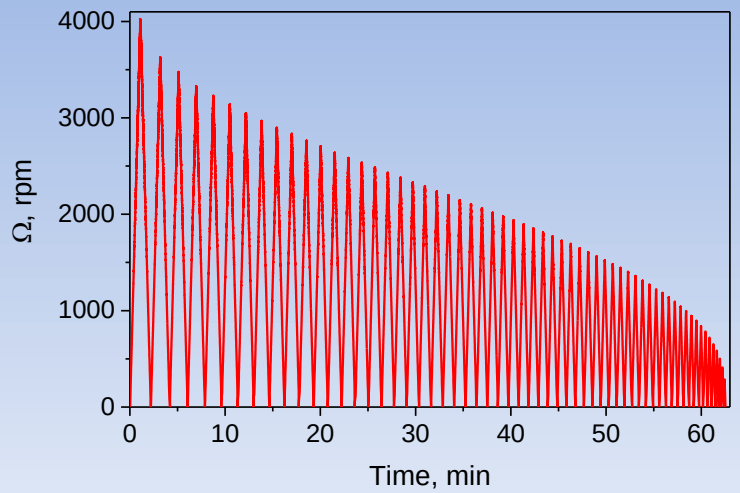

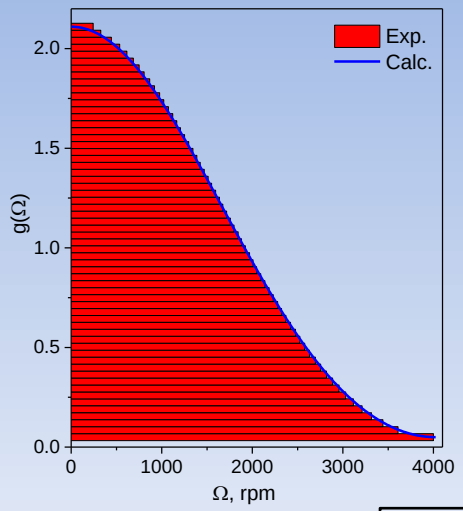

Sweep function (<u>left</u>) and frequency window (<u>right</u>) for **<u>positive</u>** composite sweep ($\Omega = 0 \div +\Omega_{max}$).

<u>Sweep functions:</u>
-Positive
-Negative
-Symmetric
-Asymmetric

$$g_i = 1 - p + q + 2 \cdot p \cdot \frac{i-1}{N-1}$$

$$g(u) = 1 + p \cdot \cos(\pi \cdot u) + q \cdot \cos(2 \cdot \pi \cdot u)$$

$$g(u) = g_i$$

$$u_i = \frac{1}{\pi} \cdot \arccos\left(\frac{-p + \sqrt{p^2 - 8 \cdot q \cdot (1 - q - g_i)}}{4 \cdot q} \right)$$

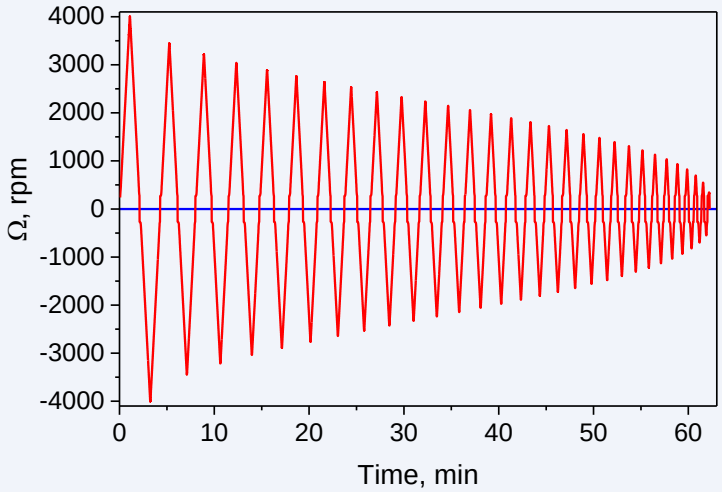

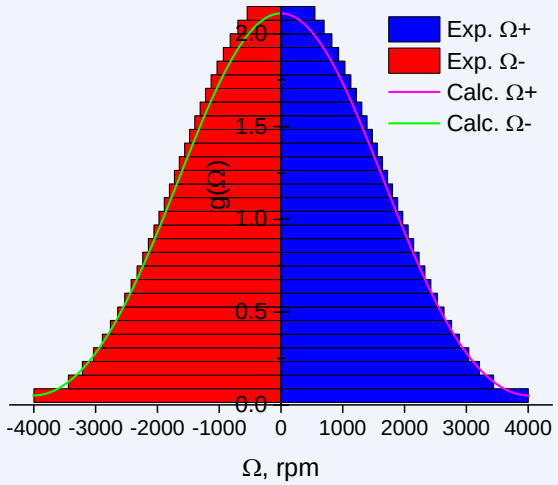

Sweep parameters: max. chopper speed Ω_{max} = 4000 rpm, exposition time t = 60 min, number of steps N = 60.

Sweep function (<u>left</u>) and frequency window (<u>right</u>) for **<u>symmetric</u>** composite sweep ($\Omega = 0 \div \pm\Omega_{max}$).

List-mode DAQ – possibilities:

- high performance and scalability of LM DAQ system;
- offline spectra reconstruction is possible without repeated measurements;
- flexibly configurable TOF-scale parameters;
- possibility to analyze: real frequency window, pickup signal, reactor starts, detector events;
- phase error correction;
- detector events filtering;
- precise electronic focusing for multi-element detectors.

2019: New Fourier chopper for FSD diffractometer by

AIRBUS DEFENCE & SPACE

Parameters:	
- Max. rotation speed	6000 rpm
- Rotor/stator material	high strength Al-alloy
- Rotor/stator thickness	4.3 mm in the slits area
- Rotor (disk) diameter	540 mm
- Rotor-stator distance	1 mm
- Slit type	real cut-away radial slits
- Number of slits	1024
- Slit length, mm	60 mm
- Slit width	0.736 mm in middle part
- Absorbing layer material	$^{10}B_4C$
- Absorbing layer thickness	0.8 mm
- Extended acceleration range	1 ÷ 300 rpm/s (cf. 10 ÷ 100 rpm/s for old chopper)

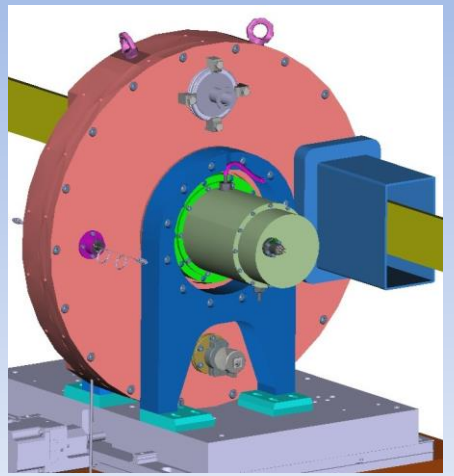

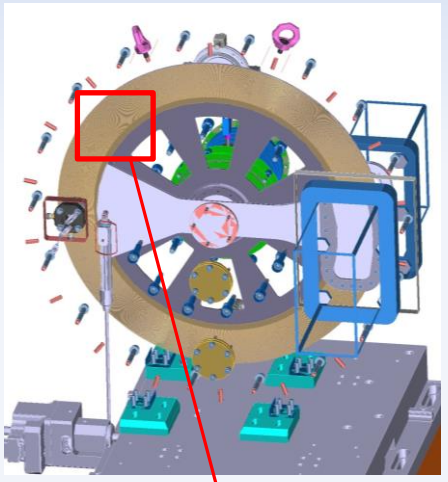

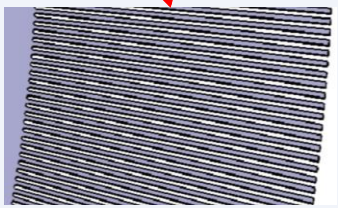

Benefits of the new design:

- Combination of two pickup systems: 1) main - laser pickup system; 2) auxiliary - optical encoder with 1024 pulses
- Direct measurement of transmission function by neutrons and by laser
- Absence of pickup shift (phase error)
- Significantly lower pickup fluctuations
- No absorption and scattering from chopper disc material
- Low gamma background
- Improved PID regulation
- Six different frequency windows
- Operation in vacuum: less vibration and higher dynamical stability

SONIX+ instrument control system
(developed in Spectrometers Complex Dept.)

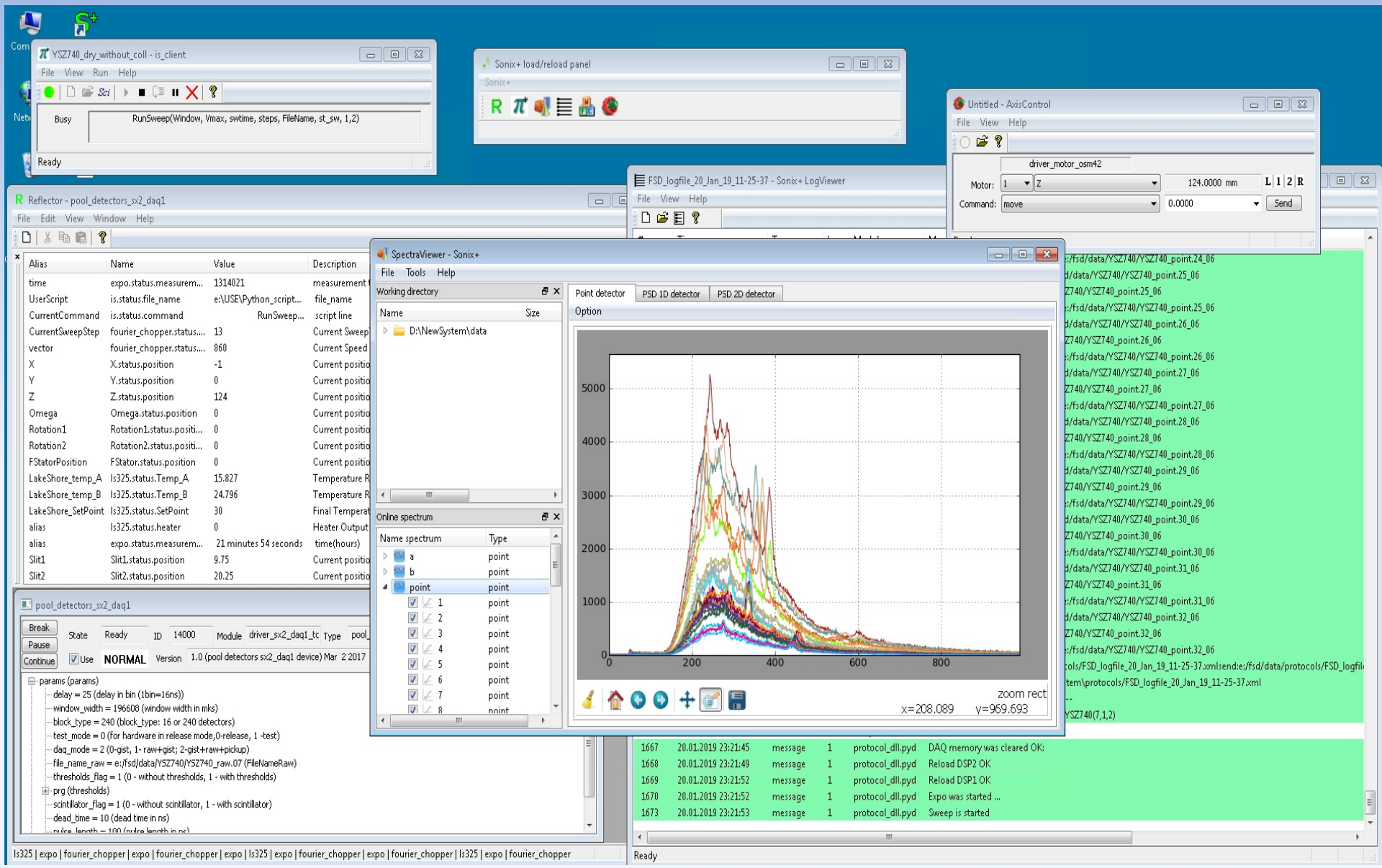

```
#######################################################
#Sample: Mg sample1.
#incident beam 8*25 mm
sd = [15,42.5,0.5,0.1]
set_diaphragm(sd[0]+0, sd[1]+0, sd[2]+8, sd[3]+25)

Sample = '_1'
m_goto(Z, 151)
#m_goto(Omega, -45)
mess_telegram('438329033', 'Start  script '+ScriptName)#igor
mess_telegram('388426679', 'Start  script '+ScriptName)#gizo
# SWEEP PARAMETERS ============================================================
SweepParameters = [4000,80,80,1,1] #[Vmax, swtime, steps, start_number_of_sweep, number_sweep]
#   fr_vin      - type of window ('asy[mmetrical]','sym[metrical]','pos[itive]','neg[ative]')
#   Vmax        - Speed max
#   swtime      - time of sweep
#   steps       - sweep's steps
# SCAN PARAMETERS ============================================================
FileMsk = 'Mg'
FileNumber = 298
Comm1 = '_Sample1_Omega='
makefoto('SampleALL',FileMsk,FileNumber)
ScanPointsList = [0,25.11,32.01,43.15,58.37,61.93,75.07,90.00] # add points to the start position
# Scan Points TXT file ========================================================
FileNum2 = FileNumber
file = open('e:\\fsd\\data\\!Script\\'+FileMsk+str(FileNumber)+'_Omega_scan.txt', "w")
file.write("Sample:\t"+Sample+"\nFileName\tOmega_scan, mm\n")
for ii in ScanPointsList:
        file.write(FileMsk+str(FileNum2)+'\t\t'+str(ii)+'\n')
        FileNum2 = FileNum2 + 1
file.close()
# RUN CURRENT SCAN ============================================================
# RUN CURRENT SCAN ==========DON'T EDIT=======================================
for i in ScanPointsList:
        if FileNumber < 100:
                if FileNumber < 10:
                        CurrFile = FileMsk+'00'
                else:
                        CurrFile = FileMsk+'0'
        else:
                CurrFile = FileMsk
        m_goto(Omega, -45+i)
        Comm = Comm1+str(i)
        protocol_dll.WriteToProtocol('File : ' + CurrFile )
        protocol_dll.WriteToProtocol('FSD INFO: Current scan point: Omega_scan='+str(i))
        RunMeas('asym',SweepParameters[0],SweepParameters[1],SweepParameters[2], SweepParameters[3],
        FileNumber += 1

mess_telegram('438329033', 'End script '+ScriptName)#igor
mess_telegram('388426679', 'End script '+ScriptName)#gizo

EndOfExperiment()
```

Experiment automation:

- Huber goniometer;
- Stress rig (load+temp.);
- Mirror furnace;
- Python user library with additional functions.

Experiment control:

- PC with RDP
- WebSONIX;
- Webcamera;
- Telegram messenger;
- Remote reset of DAQ.

Webcam for sample control

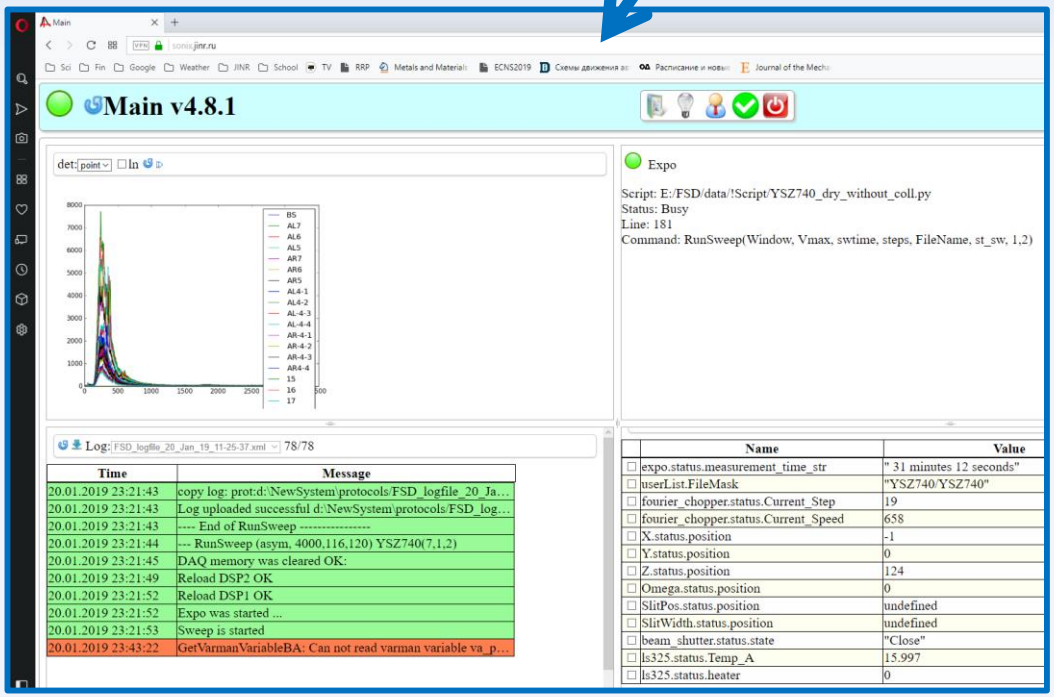

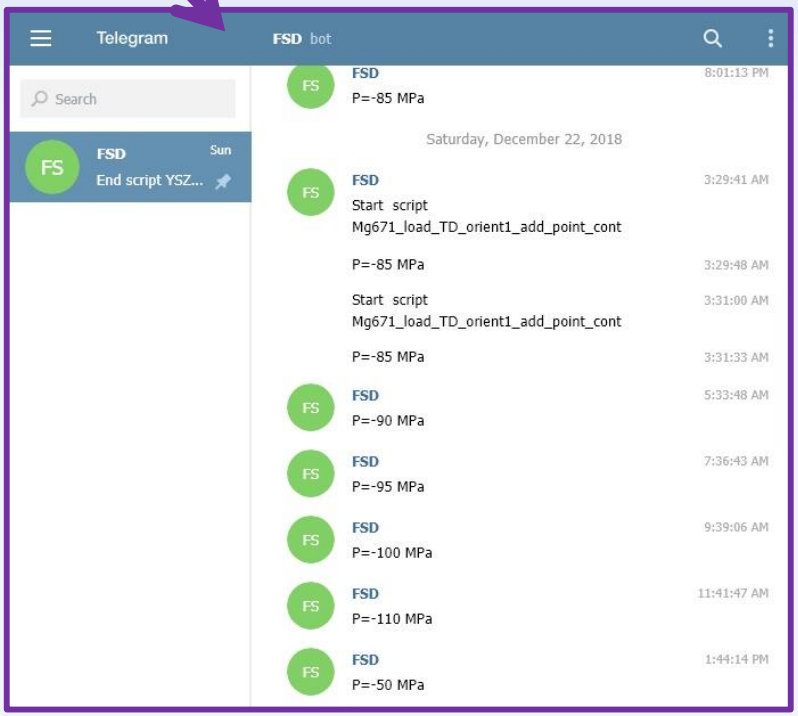

User policy @ FSD

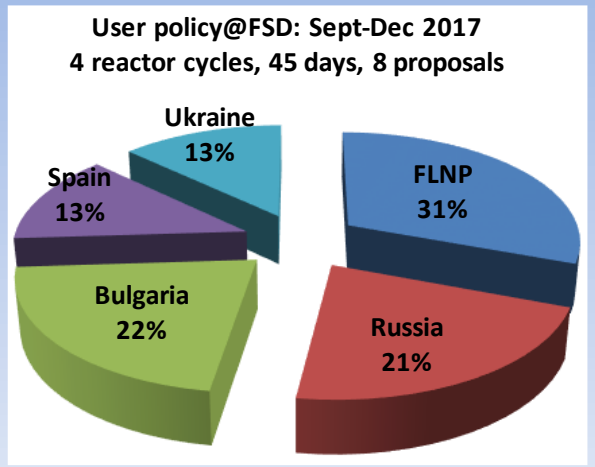

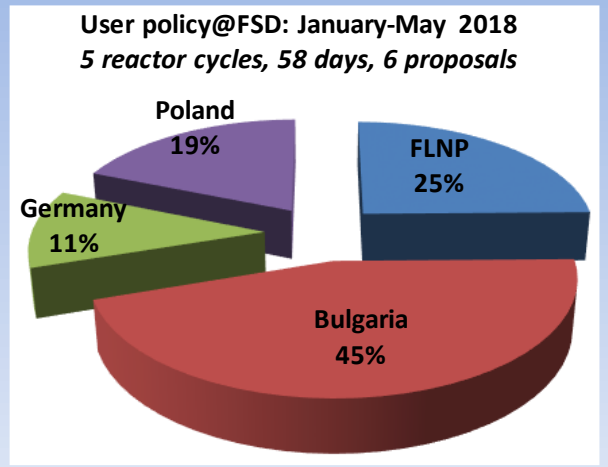

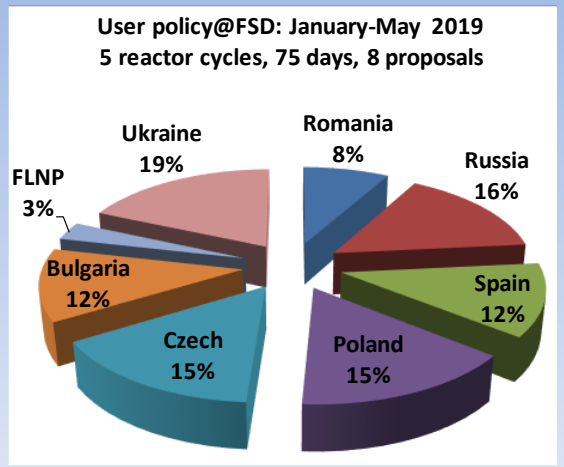

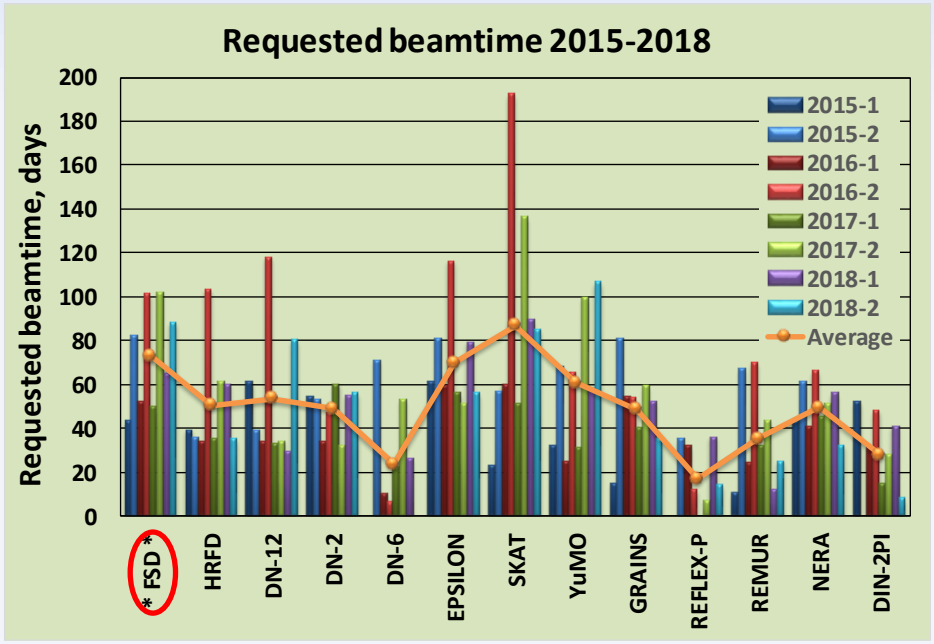

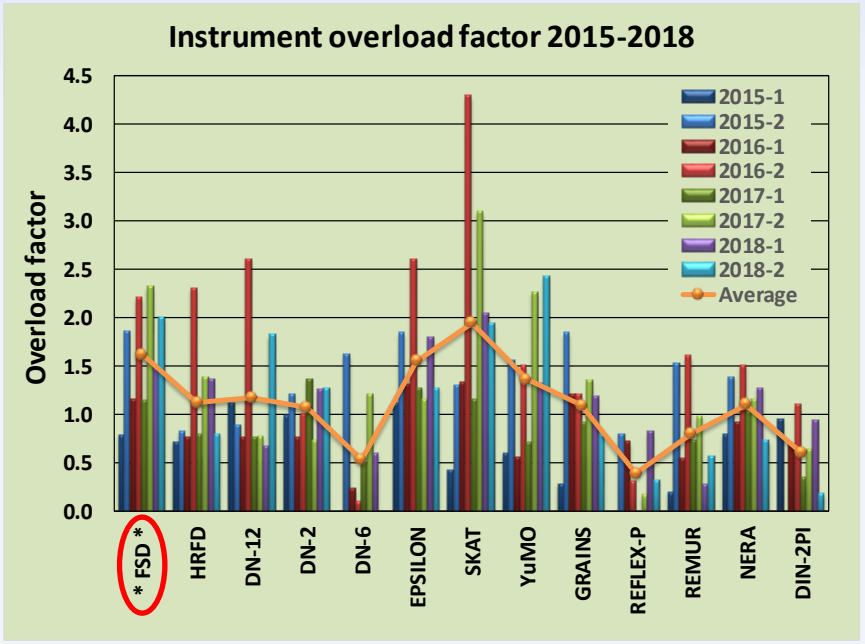

Thank you for your attention!

High-resolution Fourier diffractometry at long pulse neutron source

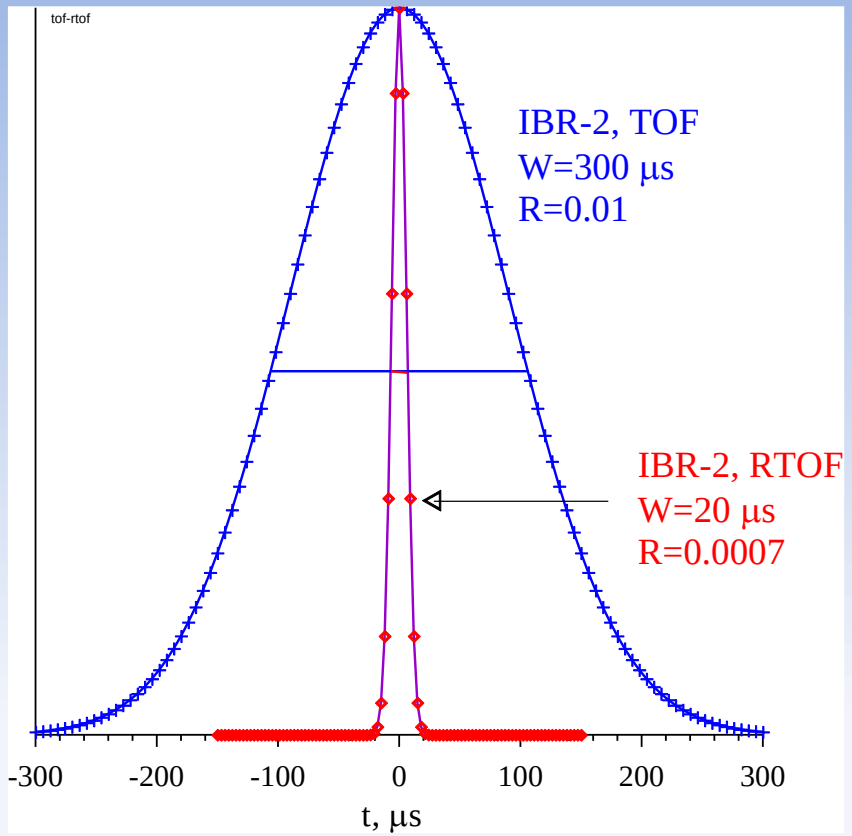

IBR-2 is a long-pulse neutron source.
Δt≈300 μs, R ≈ 0.01 = 1 % (*L*=25 m, *d*=2 Å)

Objective: R ≈ 0.001 = 0.1 % (*L*=25 m, *d*=2 Å)

Fast Fourier chopper

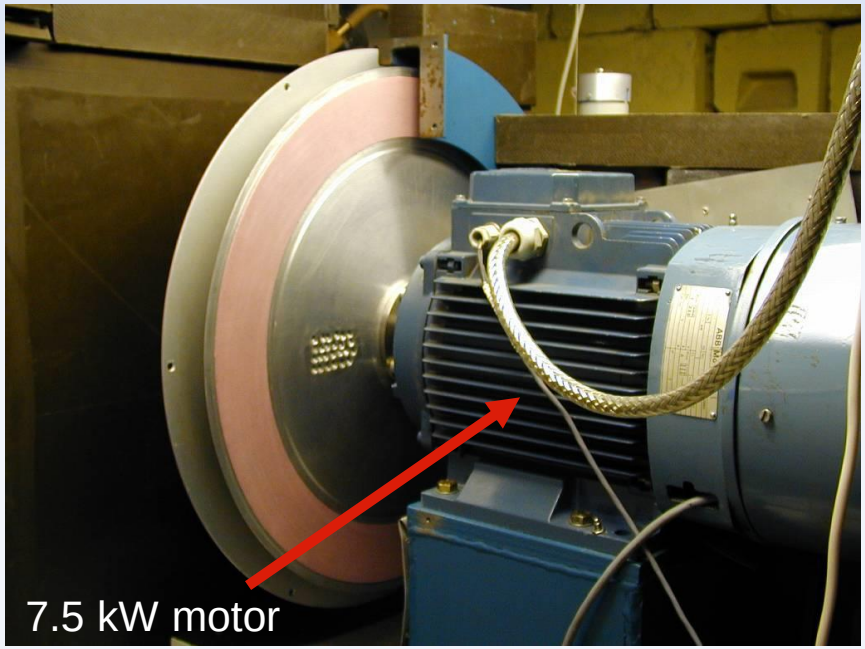

F-chopper parameters (FSD):

N=1024

V_{max}=6000 rpm

Ω_{max}=102.4 kHz

$\Delta t_0 \approx 10$ μs

P. Hiismäki; H. Pöyry; A.Tiitta. ***Exploitation of the Fourier chopper in neutron diffractometry at pulsed sources***. J. Appl. Crystallogr. 1988, 21, 349-354.

FSD diffractometer